1 9 MAR 1948

NATIONAL ADVISORY COMMITTEE FOR AERONAUTICS

WARTIME REPORT

ORIGINALLY ISSUED

August 1942 as
Advance Confidential Report

AERODYNAMIC PROBLEMS IN THE DESIGN OF

EFFICIENT PROPELLERS

By Edwin P. Hartman and Lewis Feldman

Langley Memorial Aeronautical Laboratory
Langley Field, Va.

NACA

WASHINGTON

K	Goldstein's factor
K_1	kinetic energy
M	Mach number, momentum
m	mass
n	rotational speed
P	power
P_{D_0}	profile drag power loss
P_1	induced power loss
P_L	total power loss $\left(P_{D_0} + P_1 \right)$
p	geometric pitch
Q	torque force
Q_1	torque force per blade
R	propeller tip radius, resultant force
r	station radius
S	rotational tip speed
T	thrust
T_1	thrust of single blade
V	airplane velocity
$v_1, v_2 \ldots$	arbitrary velocities
W	relative air velocity
W_0	$\tan^{-1} \frac{V}{Sx}$ (See fig. 1.)
w	effective axial inflow velocity (profile drag equal to zero)
w_1	inflow velocity

w_a axial component of inflow velocity

w_r rotational component of inflow velocity

w_2 effective rotational component in axial direction (See appendix B.)

$x =$ r/R

α angle of attack

α_0 angle of attack for infinite aspect ratio

α_i induced angle of attack

β blade angle

η section efficiency

η_a axial induced efficiency

η_r rotational induced efficiency

$\Delta\eta$ efficiency loss $= 1 - \eta$

η_p propulsive efficiency

η_i induced efficiency (profile drag equal to zero)

ρ mass density of air

ρ_0 mass density of air at sea level

σ section solidity $\left(\sigma = \dfrac{bB}{2\pi r}\right)$

ϕ angle of relative-air-speed vector to propeller disk (helix angle of wake)

$\phi' =$ $\tan^{-1}\dfrac{V}{2\pi rn} = \tan^{-1}\dfrac{V}{Sx}$ (helix angle of propeller)

Figure 1 illustrates some of the symbols. The foot-pound-second system is used except where noted.

I. BLADE LOADING FOR MINIMUM INDUCED-ENERGY

LOSS - PROFILE DRAG NEGLECTED

General Analysis.

Attempts have been made to determine analytically the blade loading that will give a minimum loss of energy for a given thrust. From original calculations by Goldstein and Betz, Lock and Bateman (reference 1) have developed formulas from which the loading giving the minimum energy loss (profile drag being neglected) may be obtained for lightly loaded propellers. Inasmuch as a propeller has a relatively light loading at maximum efficiency, it is believed that the Goldstein theory will hold for efficient propellers in the high-speed condition.

Propellers with the optimum loading (called Betz propellers herein) have been designed and tested in Great Britain. The British tests of reference 1 show a maximum propeller efficiency of 93.2 percent for a Betz propeller, an efficiency 3 percent higher than the efficiency of any other propeller of a fairly large group tested. The purpose of part I of this paper is to show how the loading that gives the minimum induced-energy loss can be obtained from rather elementary considerations and to present design charts from which such a plan form can be quickly obtained for any set of design conditions.

One characteristic of a propeller of optimum loading is that all sections along the blade operate at the same efficiency. With the condition imposed that a propeller blade shall produce a given thrust, the blade may be designed to have any desired radial distribution of thrust. The highest efficiency will be obtained when the thrust distribution is such that all sections operate at the same efficiency. If one section of a propeller is operating at a higher efficiency than the other sections, an increase in over-all efficiency will be obtained by shifting some of the load from the less efficient sections to the more efficient sections. In the end, the efficiency will be equalized over the whole blade because the section efficiency decreases as the section load is increased.

The discussion of appendix A shows that, when the profile drag is assumed to be zero, the condition for constant induced efficiency along the blade is specified by the fact that the effective inflow velocity w is constant. (See fig. 1.) Under these conditions, the sheet of vortices shed by each blade moves backward as a rigid helix.

6

The inflow velocity, $w_1 = W \cos \phi$, is produced (when profile drag is neglected) by the lift force alone and is therefore shown in figure 1 to be at right angles to the relative air velocity W.

Appendix B shows that

$$w_1 = \frac{\sigma C_L W}{4K \sin \phi}$$

where K is a factor, determined by Goldstein, that accounts for the difference in inflow velocity between propellers with an infinite and a finite number of blades. Goldstein's original determinations of K covered only a relatively small range, which has been greatly expanded by Lock and others. The value of K varies with the number of blades, the value of x, and the angle ϕ. Plots of K against $\sin \phi$ with the parameter x, given in reference 2 for two-, three-, and four-blade propellers, have been reproduced in this report as figures 2, 3, and 4.

The condition that the wake moves backward as a rigid helix can be expressed mathematically as

$$x \tan \phi = \text{a constant}$$

This condition, the aerodynamic pitch of the propeller being constant, is the one fundamental criterion for the propeller of minimum induced loss, the Betz propeller. Appendix B further shows that, when $x \tan \phi$ is a constant and when B, n, D, and V are specified, the product bC_L becomes a specific function of x. An approximate relation developed by Lock and Bateman and confirmed in appendix B is as follows:

$$bC_L \approx kK \sin \phi \cos^2\phi \qquad (1)$$

The necessary condition that $x \tan \phi$ be constant along the blade may be written

$$k_1 x = \cot \phi \qquad (2)$$

The following two equations, therefore, result for any particular design:

$$bC_L \approx kK \sin \phi \cos^2\phi$$

$$k_1 x = \cot \phi$$

where k and k_1 are constants and K is given as a function of $\sin \phi$, x, and B in figure 2, 3, or 4.

With equations (1) and (2) and the values of K from figure 2, 3, or 4, bC_L/k can be plotted against x, with k_1 as a parameter, for the two-, three-, and four-blade propellers for which values of K are available. When bC_L/k is divided by its value at $x = 0.7$, plots of $bC_L/bC_{L_{x=0.7}}$ against x, with k_1 as a parameter, may be made.

The process just mentioned has been carried out to obtain the families of Betz loadings for two-, three-, and four-blade propellers; these families are given in figures 5, 6, and 7. The calculations were made for values of the parameter k_1 of 1, 1.5, 2, 3, and 4, which in the figures have been interpreted in terms of the angle ϕ at $x = 0.7$ by means of equation (2). The values of ϕ are given to the nearest $0.5°$. For many designs, however, it may prove advantageous to work out the distributions from basic considerations rather than from interpolated values from the charts.

The angle ϕ is not explicit in the design information. Its relation to more commonly used angles in propeller design is therefore given to provide a better understanding of the figures. The angle ϕ is greater than $\tan^{-1} \dfrac{V}{\pi n D x}$ by the amount of the induced angle α_1, which is usually between $1°$ and $2°$ in the high-speed case. Furthermore, the angle ϕ is less than the blade angle by the amount of the angle of attack α_0 measured from the same reference line.

Discussion of Figures

Several significant features should be pointed out in figures 5 to 8. It will be noticed in figures 5, 6, and 7 that, as the angle ϕ increases, the loads (bC_L) on the inboard sections become smaller with respect to the loads on the outboard sections. The shape of the loading of a Betz propeller is determined by the consideration of making the best compromise between induced tip losses and rotational losses. As the value of $\phi_{x=0.7}$ increases, the angles in the shank sections and therefore the rotational losses of the shank sections increase; in order to balance this tendency toward loss, some of the load is shifted toward the tip. At low blade angles, the effect of induced tip losses predominates and the load is shifted toward the shank. The best compromise is secured in all cases.

In the case of coaxial counterrotating propellers, the design of which is not considered in this report, the rotational energy (losses) imparted to the slipstream by the front propeller is partially recovered by the rear propeller, and the net rotational loss of the propeller combination is thus greatly reduced. Therefore, as the rotational-loss factor for coaxial counterrotating propellers is less important than for single-rotating propellers, a considerable difference will exist between the optimum loadings for these two types of propellers. The optimum loading for a counterrotating propeller will call for much heavier loads on the inboard sections and somewhat lighter loads on the tip sections than in the case of a single-rotating propeller.

Figure 8 shows a comparison between loading curves for Betz propellers of two, three, and four blades at $\phi_{x=0.7} = 35.5°$. As the number of blades decreases, the center of the load shifts toward the shank. This characteristic is the result of the higher induced tip loss of propellers with fewer blades. The design of Betz propellers is so intimately related to induced losses that the inclusion of a brief discussion of induced tip loss was considered desirable. That discussion may be found in appendix C.

Application of Data

When differential thrust $\dfrac{dT_1}{d(x)^2}$ is plotted against x^2, a curve of approximately semielliptical shape is produced. If the curve were exactly semielliptical, the following exact expressions for the total thrust of the blade in terms of the elementary thrust at station $x = 0.7$ could be written:

$$\left(\frac{dT_1}{d(x)^2}\right)_{x=0.7} = \frac{4}{\pi} T_1$$

and, as

$$\frac{dT_1}{d(x)^2} = \frac{dT_1}{2x\,dx}$$

then

$$\left(\frac{dT_1}{dx}\right)_{x=0.7} = 1.4 \times \frac{4}{\pi} T_1 = 1.78\,T_1 = aT_1$$

where a represents the constant 1.78.

Experience has shown, however, that the ellipticity of the thrust distribution of a propeller varies with the design value of J and that the value of a varies accordingly. For optimum propellers, the general trend in the variation of a with J is indicated in the following table.

TABLE I

Design J	a
1.0	1.61
1.5	1.73
2.0	1.79
2.5	1.83
3.0 to 4.0	1.85

Now, inasmuch as

$$T_1 = \frac{550 \times hp \times \eta_p}{VB}$$

and

$$\left(\frac{dT_1}{dx} = RbC_L \frac{\rho W^2}{2} \cos \phi \right)_{x=0.7}$$

substitution yields

$$\left(RbC_L \frac{\rho W^2}{2} \cos \phi \right)_{x=0.7} = \frac{550 \times hp \times \eta_p \times a}{VB}$$

Then, because $W \approx \frac{V}{\sin \phi}$, the following evaluations can be made:

$$\left(bC_L \right)_{x=0.7} \approx \frac{2200 \times hp \times \eta_p \times a}{\rho V^3 BD} \left(\frac{\sin^2 \phi}{\cos \phi} \right)_{x=0.7} \tag{3}$$

and, assuming $\phi = \phi'$,

$$\left(\frac{bC_L}{D} \right)_{x=0.7} \approx \frac{0.827 \times C_p \times \eta_p \times a \, (\cos \phi)_{x=0.7}}{BJ} \tag{4}$$

In any normal design, B, P, ρ, V, and n will be specified; η_p can then be estimated or obtained from figure 9, D can be estimated from propeller selection charts, J can be computed, and a can be selected from table I.

The value of diameter estimated from propeller selection charts will probably not be, exactly, the optimum diameter. The optimum value of D is difficult to determine. In some cases it is fixed by tip-speed limitations or by tip clearance with the ground. A discussion of the aerodynamic aspects of the problem of selecting the optimum diameter for a propeller is given in appendix D.

Figures 5, 6, and 7 give families of Betz loadings with the product $\dfrac{bC_L}{(bC_L)_{x=0.7}}$ as a function of x. It is significant that the plan form corresponding to a Betz loading is not fixed but may be varied by changing the lift coefficient along the blade. The adjustable nature of the components, b and C_L, of bC_L is the basis for the profile-drag analysis in part II of this paper.

It is of importance to note that the Betz propeller has a definite aerodynamic pitch which can be easily determined after one value of ϕ at any place along the blade has been determined. (See equation (2).) The blade angle distribution can then be quickly ascertained once the distribution of lift coefficient (and consequently angle of attack) is known from the following relations:

$$\beta = \phi + \alpha$$

where α is the angle of attack required to obtain the desired lift coefficient. From equation (2)

$$x \tan \phi = \frac{1}{k_1}$$

and

$$\phi = \phi' + \alpha_1$$

where

$$\phi' = \tan^{-1} \frac{V}{Sx}$$

we can determine ϕ_x if we can determine α_1.

The value of α_1 is small for normal high-speed design so that the angle may be substituted for its sine. Therefore, in radians,

$$\alpha_1 = \sin \alpha_1 = \frac{\sigma C_L}{4K \sin \phi} \qquad (5)$$

The value of α_1 may be determined with good accuracy by making the substitution $\sin \phi = \sin (\phi' + 2^\circ)$ in equation (5) and by using the same approximation for $\sin \phi$ in obtaining K from figure 2, 3, or 4. The value of α_1 at $x = 0.7$ is, therefore,

$$\alpha_{1_{x=0.7}} = \frac{57.3 \, (\sigma C_L)_{x=0.7}}{4K \sin \left(\phi'_{x=0.7} + 2.0^\circ\right)} \text{ degrees}$$

and

$$\alpha_{1_{x=0.7}} = \frac{6.5 \, B \, (b C_L)_{x=0.7}}{DK \sin \left(\phi'_{x=0.7} + 2.0^\circ\right)} \text{ degrees} \qquad (6)$$

where

$$\phi'_{x=0.7} = \tan^{-1} \frac{V}{0.7\pi n D}$$

$$= \tan^{-1} \frac{V}{0.7S} \qquad (7)$$

II. PROFILE DRAG CONSIDERATIONS

Power Loss at Any Section

In the case of a general propeller operating under specified conditions, the induced losses are fixed for a given diameter, blade number, and load distribution and are a minimum if the loading is the Betz loading for the specified conditions. The only changes in efficiency that can be effected are those due to profile drag, and these changes occur in two ways: first, as a direct power loss and second, as a correction to the induced loss due to the distortion of the wake. The familiar assumption that induced effects act independently of profile drag suggests that the effect of the distortion is small and that it may be neglected.

Inasmuch as the profile-drag power loss is, in the case just mentioned, the only variable susceptible to design treatment (optimum loading having been assumed), considerable importance attaches to its effects on performance and design and especially to its effect on plan-form design. It is the purpose of this section to show how intimately profile-drag considerations are involved in optimum plan-form determination.

If it is assumed that the distortion of the wake resulting from profile drag has but a negligible effect on induced efficiency, the over-all efficiency of a propeller having a Betz loading will be a maximum when the profile-drag loss of each section is as low as possible. The expression for the profile-drag power loss is

$$dP_{D_0} = RB \ bC_{D_0} \frac{\rho}{2} W^2 \ dx \ (V \sin \phi + Sx \cos \phi) \tag{8}$$

Now

$$V \sin \phi' + Sx \cos \phi' = W_0$$

and as

$$\phi \approx \phi'$$

and

$$W \approx W_0$$

$$dP_{D_0} = RB \ bC_{D_0} \frac{\rho}{2} W_0^3 \ dx$$

and

$$\frac{dP_{D_0}}{dx} = RB \ bC_{D_0} \frac{\rho}{2} \frac{V^3}{\sin^3 \phi'} \tag{9}$$

where W_0, V, R, and ρ are fixed for the specified case.

Equation (9) includes the differential power loss $\left(\dfrac{dP_{D_0}}{dx} \right)_Q$ resulting from the torque component of the profile drag as well as the differential power loss $\left(\dfrac{dP_{D_0}}{dx} \right)_T$ resulting from the thrust component of the profile drag. It may be easily shown that

$$\frac{\left(\dfrac{dP_{D_0}}{dx}\right)_T}{\dfrac{dP_{D_0}}{dx}} = \sin^2\phi'$$

and

$$\frac{\left(\dfrac{dP_{D_0}}{dx}\right)_Q}{\dfrac{dP_{D_0}}{dx}} = \cos^2\phi'$$

It is clear then that $\left(bC_{D_0}\right)_{min}$ is the condition for minimum profile-drag loss at any section. Because the quantity bC_{D_0} is the lone parameter affecting profile-drag losses, its position and relation to other quantities should be clearly understood.

As a result of the complicated interrelationships of the quantities affecting bC_{D_0}, it becomes necessary to simplify the problem by making certain assumptions. It will be assumed that the absolute thickness distribution required can be predicted from previous designs. This assumption can be made valid by successive approximations. It will further be assumed that variations in blade width can be made without affecting the thickness requirements. The aerodynamic factors affecting the bC_{D_0} at any station are:

1. Airfoil section

2. Lift coefficient or camber

3. Section chord

4. Section thickness

5. Mach number

The determination of the optimum plan form is, in fact, nothing but the adjustment of the airfoil section, the camber, and the section chord as dictated by section thickness, Mach number, and the required loading (bC_L) in order to achieve the minimum drag $\left(bC_{D_0}\right)$. In traditional blade design, the airfoil section family is selected (for example, Clark Y) and the specific section is determined by the

thickness ratio. In such a case, there can be no independent variation of camber and thickness ratio. The operating lift coefficient is realized by adjustment of the angle of attack, and no provision is therefore made to permit the blade sections to operate at their optimum lift coefficients. Thus, the conflicting conditions of high thickness ratios and low lift coefficients (at inboard stations), and vice versa, lead to large positive or negative angles of attack and the accompanying increases in profile-drag coefficient.

A new propeller section (the 16-series airfoil) has been developed recently at the NACA (reference 3) which, from preliminary tests, appears to be much better suited to propellers for high-speed airplanes than any other known sections. The new sections have very low profile-drag coefficients and late compressibility stalls for their design lift coefficients. The curvature of the mean camber line, independent of thickness ratio, is a function of the design lift coefficient, which may be selected to fit the operating conditions. It has been found that the minimum profile-drag coefficient attainable for a given thickness ratio and lift coefficient occurs for the section designed to operate at that lift coefficient. When the 16-series family (or any other family similarly derived) is used, the camber and the blade width can be adjusted to yield minimum drag at any station where the lift load, thickness, and Mach number are known.

At a given station the product bC_L is held to a constant value arrived at from the induction considerations of part I. Decreases in blade width then necessitate increases in camber that are accompanied by increases in profile-drag coefficient. The net effect on the section drag index bC_{D_0} depends on the magnitude of the change in b and the associated variation of C_{D_0} with camber (C_L).

Similarly, if the section thickness is constant, as previously assumed, decreases in blade width cause increases in thickness ratio and corresponding increases in drag coefficient. These reciprocal actions hint at the existence of an optimum blade width such that the balance of blade width (b) against profile-drag coefficient yields a minimum value of bC_{D_0}. These reciprocal actions also indicate that "optimum plan form" is just one aspect of "best blade shape," which includes the distribution of camber and thickness ratio.

Determination of Best Blade Shape

The problem involved in finding the best blade shape is the determination of the values of b, C_L, and h/b that will yield the minimum value of bC_{D_0}. If a plot of C_{D_0} against C_L is made for a family of airfoils with the operating C_L equal to the design C_L and with the thickness ratio varied as a parameter, curves of the type shown in figure 10 result. Thickness ratio increases from $(h/b)_1$ toward $(h/b)_5$.

In a given case, where $bC_L = k_3$ and $h = k_4$, any value of C_L determines a value of $b = \dfrac{k_3}{C_L}$ and a value of $\dfrac{h}{b} = \dfrac{k_4 C_L}{k_3}$ and therefore a point on the plane of figure 10. Then, inasmuch as C_L can have any value in that plane, the conditions $bC_L = k_3$ and $h = k_4$ determine a line in that plane. Such a line is $A_1 - A_2$. Every point on that line has a single value of C_L, b, h/b, and C_{D_0}. If these values are combined, each point on line $A_1 - A_2$ can be plotted as a point of bC_{D_0} against b (or C_L). The resulting curve will show the variation of section drag with chord and the values of b and C_L for minimum bC_{D_0} will be indicated. Plots of this type are shown in figure 11.

Inasmuch as this procedure involves the profile-drag coefficient, it is dependent on wind-tunnel data. The data required are currently being made available but as yet are incomplete. It must be kept in mind that, because C_{D_0} is strongly affected by compressibility, data taken at the proper Mach number must be used.

The Effect of Compressibility on Plan Form

The effects of thickness ratio and of lift coefficient on the critical speed of an airfoil section have been determined by theory and verified by experiment (reference 3). The results of the investigation show characteristic curves such as curves illustrated in figure 12. It is apparent from the curves that, for a given Mach number and a given thickness ratio, there is a maximum allowable lift coefficient compatible with subcritical drag coefficients. These airfoil data, however, are not applicable to the tip portions of propellers because tip effects appear to delay the compressibility burble.

If propeller wake-survey data at high speeds are analyzed as curves of critical Mach number at known lift coefficients and thickness ratios, these curves have the same shape as airfoil critical-speed curves but are shifted to higher Mach numbers. Accurate data in this form are needed for this type of analysis and are currently being made available. As only limited tests have yet been run (reference 4), data for only one thickness ratio and one airfoil section are obtainable. (See fig. 13.)

At a given station of some known propeller, the Mach number is known. For any thickness ratio, then, the maximum allowable lift coefficient and its complement, the minimum required blade width, are fixed. This minimum required blade width is not necessarily the optimum blade width. It is only the minimum blade width required to avoid exceeding the critical speed for the given conditions.

This concept, however, is most valuable if these considerations are reversed. If the thickness ratio and the blade width are fixed by structural considerations at some values, the maximum allowable tip speed can be evaluated. With maximum allowable tip speed known, the largest diameter (and therefore the lowest induced loss) can be computed.

The direct evaluation of minimum blade width required is unnecessary. Data such as that of figure 13 can be plotted on figure 14 and will appear as a line similar to $B_1 - B_2$ of figure 10 at the break in the drag curves. Because of the precipitous rise in C_{D_0}, the blade width for minimum bC_{D_0} will always be greater than the minimum blade width required.

III. EXAMPLE

A simplified example will be carried through to show the use of the methods outlined in parts I and II for obtaining propellers of optimum aerodynamic design. Calculations will be made for the Betz loading and then for the optimum plan form determined by the loading, the thickness distribution, and the profile drag. No effort will be made to design a structurally satisfactory propeller, but the structural necessities of the propeller are considered by the use of the thickness distribution of a known propeller of the same capacity.

Moderate forward speed and moderate tip speed shall be assumed
for this example in order that tip considerations may not demand
unavailable data. The curve of figure 13 is presented for purposes
of illustration only and should not be used too generally. This
condition is also true of figure 14, which has been constructed and
faired from uncorrected data. The trends in both figures are
correct, however, and their values are approximately right. The
design conditions assumed for this example are:

P, horsepower 1200
n, rps 25
V, feet per second 440
D, feet 11.5
B 3
Altitude . . . . sea level

Sections of the NACA 16 series and the limited data available will
be used.

Determination of Optimum Loading

The estimation of the value of the angle ϕ is a logical
starting point from which to begin the determination of the optimum
loading.

If the method indicated in part I is followed,

$$S = \pi n D = 904 \text{ feet/second}$$

In equation (7), it is shown that

$$\tan \phi'_{x=0.7} = \frac{V}{0.7S}$$

$$\tan \phi'_{x=0.7} = \frac{440}{0.7 \times 904} = 0.695$$

$$\phi'_{x=0.7} = 34.80°$$

Inasmuch as a value of α_1 must be assumed in order to calculate ϕ,
the value $\alpha_1 = 2°$ is used and then this value is checked later.

$$\sin \phi_{x=0.7} = \sin \left(\phi'_{x=0.7} + 2°\right) = \sin 36.80° = 0.599$$

$$\cos \phi_{x=0.7} = 0.801$$

18

From equation (3):

$$\left(bc_L\right)_{x=0.7} = \frac{2200 \times bp \times \eta_p \times a}{\rho V^3 \; BD} \left(\frac{\sin^2\phi}{\cos\phi}\right)_{x=0.7}$$

In this example, the value of a is arbitrarily taken as 1.875^* and, from figure 9,

$$\eta_p = 0.85$$

Therefore

$$\left(bc_L\right)_{x=0.7} = 0.271 \text{ ft} = 3.25 \text{ in.}$$

From equation (6)

$$\alpha_{1_{x=0.7}} = \frac{6.5 \; B \; \left(bc_L\right)_{x=0.7}}{DK \sin \phi_{x=0.7}}$$

$$= \frac{6.5 \times 3 \times 0.271}{11.5 \times 0.65 \times 0.599} = 1.18^\circ$$

The effect on $\sin \phi$ of the assumption of $\alpha_1 = 2^\circ$ will be shown by recalculating bc_L, ϕ, and α_1 where

$$\alpha_{1_{x=0.7}} = 1.18^\circ$$

New value of $\phi = (\phi)'_{x=0.7} = 35.98^\circ$

$$\sin (\phi)'_{x=0.7} = 0.588$$

$$\cos (\phi)'_{x=0.7} = 0.809$$

---

*As this example was worked out before the quantitative value of the variation of a with J was established, the value of 1.875 for a was arbitrarily chosen. A somewhat more appropriate value, 1.75, might now be selected from table I.

New value of $\left(bC_L\right)_{x=0.7} = \left(bC_L\right)'_{x=0.7} = \left(bC_L\right)_{x=0.7}\left(\dfrac{\sin(\phi)'}{\sin\phi}\right)^2 \Big/ \dfrac{\cos(\phi)'}{\cos\phi}$

$$= 0.271\left(\dfrac{0.588}{0.600}\right)^2 \Big/ \dfrac{0.809}{0.800}$$

$$= 0.260$$

New value of $\alpha_1{}_{x=0.7} = \left(\alpha_1\right)'_{x=0.7} = 1.145°$

and from appendix A, the induced efficiency

$$\eta_1 = \frac{\tan\phi'}{\tan\phi} = \frac{\tan 34.8°}{\tan 35.95°} = 0.96$$

The difference between the recalculated and original values of α_1 and bC_L would seem to justify the effort involved in the recalculation.

With $\tan\phi$ now known as $\tan(\phi' + \alpha_1)$ at $x = 0.7$ and with

$$x\tan\phi = \frac{1}{k_1} \tag{10}$$

where

$$\frac{1}{k_1} = 0.7\tan(34.80° + 1.145°)$$

$$= 0.7\tan(35.95°)$$

$$= 0.7 \times 0.725 = 0.507$$

the value of ϕ can be found at any station simply by substituting x in equation (10). The value of $\phi_{x=0.7}$ determines a particular curve of $bC_L/bC_{L_{x=0.7}}$. Table II shows convenient tabulations of basic propeller factors and computations of the bC_L curve for this particular example to show the computations involved in the construction of figures 5, 6, and 7.

Determination of Optimum Blade Width

In order to begin the evaluation of the blade width, a thickness distribution must be assumed. For this example, an average thickness distribution was taken from commercial propellers currently being used.

(See fig. 15.) The propeller calculated on the basis of this assumption will not necessarily be structurally satisfactory. On the other hand, if the blade width distribution of the propeller is not too different from regular plan forms, its structural properties may be easily adjusted. It is believed that the empirical selection of the thickness distribution will not detract from the practical nature of the computations.

The computation of the blade width for a given section with h, bc_L, and M known requires but a few simple steps, as follows:

1. Compute the value of b corresponding to the thickness h for each of the h/b ratios on figure 14.

2. Compute $c_L = bc_L/b$ for each of the values of b computed in step 1.

3. Locate the points determined by h/b and c_L on figure 14 and find the corresponding values of c_{D_0}.

4. Plot bc_{D_0} against c_L from data in step 3 to locate $\left(bc_{D_0}\right)_{min}$.

5. From the value of c_L for $\left(bc_{D_0}\right)_{min}$ compute b_{opt}.

It is important to notice that the data such as in figure 14 must be at the proper Mach number for each section. In this example data from figure 14 $(M = 0.60)$ is used for all stations irrespective of speed differences. The effect of this simplification will be discussed. Table III and figures 11 and 16 show the operations carried out.

The curves in figure 11 show some very interesting results. For most of the stations analyzed, the optimum thickness ratio is around 9 percent with thickness ratios of 6 percent showing definite detrimental effects on profile drag. In addition, the drag of sections with thickness ratios of 12 percent is consistently lower than the drag of sections with 6-percent thickness ratios. The drag of a 6-percent-thick section is about equal to the drag of a 15-percent-thick section with the same absolute thickness. It should be remembered that in a practical design the thickness may need adjustment. The indicated results, however, are approximately correct.

The drag data from which these curves were plotted were all obtained at a Mach number of 0.600. Inasmuch as the Mach number varied from 0.464 at $x = 0.3$ to 0.866 at $x = 0.95$, the results

are not exactly conclusive. The effect of the increase in Mach
number from root to tip would be to decrease the blade width at
the root and to increase it at the tip. The blade width and lift-
coefficient curves of figure 16 are based only on high-speed
performance. In order to compromise for take-off and climb
performance, the design C_L values (camber) of the root sections
would probably be increased to give higher values of $C_{L_{max}}$ for
those sections. The results of figure 11 show that cuffs may be
desirable even for propeller installations with large spinners.

Comparison of Results

In order to evaluate the importance of the effects of change
in plan form on the profile-drag losses, calculations of profile-
drag power loss were made for two blades: one blade having the
calculated optimum plan form, and the other having conventional
blade form. It is difficult to evaluate accurately the drag
coefficient of an operating propeller section, particularly when
the loading is unknown. The following estimations of profile-
drag power loss may not, therefore, correspond to the actual
absolute power loss. The comparative values of the two estimations,
however, should be accurate.

In an earlier section of this report, the following relation
for the differential profile-drag power loss was given:

$$dP_{D_0} = RB \; bC_{D_0} \; \frac{\rho}{2} \; W_0^3 \; dx$$

and

$$\frac{dP_{D_0}}{dx} = RB \; bC_{D_0} \; \frac{\rho}{2} \; \frac{V^3}{\sin^3 \phi}$$

Then

$$\frac{\dfrac{dP_{D_0}}{dx}}{B} = \frac{bC_{D_0}}{\sin^3 \phi} \; k_5$$

where

$$k_5 = \frac{\rho R \; V^3}{2}$$

Figure 17 shows the curves of profile-drag power loss along the blade, $\dfrac{dP_{D_o}}{dx}\Big/B$, and the value of the integrated power loss for each case.

Also included in figure 17 is a curve of $\dfrac{dP_i}{dx}\Big/B$ for the optimum propeller. Thus a comparison of the induced and the profile-drag power loss is provided for this propeller. The profile-drag power loss of the standard propeller is 33.25 horsepower per blade or 8.3 percent of the total power per blade for the portion of the blade examined. The blade that has camber and blade width adjusted to optimum conditions has a corresponding loss of 12.27 horsepower per blade or only about two-fifths as much. The total net indicated advantage is then 5.23 percent of the total power input.

It must again be mentioned that these figures are obtained on the basis that the sections are designed to operate at fixed lift coefficients. This condition allows the blade width to be determined in the light of separate but concurrent considerations of thickness ratio and camber. If the plan form is made optimum for sections varying only in thickness ratio or if the sections are selected for minimum drag coefficient without reference to blade width, the whole benefit outlined herein cannot be gained.

Although it is true that the indicated gains arising from the use of the optimum design may not be fully realized because of practical limitations on blade shape and size, the evidence provided by the comparison is, nevertheless, important in that it points out the gains that can be made if fabrication and structural problems are solved.

The propulsive efficiency of a propeller operating in front of a well-streamlined body need not be seriously affected by body interference because the loss in propeller efficiency may be partly compensated by a lower pressure drag (form drag) of the body in the slipstream.

The pitch distribution of a propeller designed for free-air operation should be altered when the propeller is used in the presence of a body. The alterations require a knowledge of the velocity field in the plane of the propeller. The velocity field can be obtained by velocity surveys or, for certain shapes, it can be calculated.

The load distribution for the altered propeller may be made the same as for the free-air design or it may be made somewhat lower over those sections affected by the increased airspeed. The best loading for this case is not known; the body influence, however, may affect only the less important (inboard) sections. Three-quarters, or more, of the thrust is generally produced by the outer half of the blade, where, for fine-nosed bodies, the body influence on the air flow will be negligible.

CONCLUDING REMARKS

The present work gives practical methods for obtaining (1) the optimum blade loading for the case when profile drag is assumed to be zero and (2) the best blade shape when profile drag is present but is assumed to act without changing the induced efficiency. The theoretical bases for the two methods are also given. The use of the method is at present limited by insufficient aerodynamic section data. It is shown that the profile drag of the propeller sections has a large influence on the blade shape for maximum efficiency.

Langley Memorial Aeronautical Laboratory,
    National Advisory Committee for Aeronautics,
        Langley Field, Va.

APPENDIX A

AN ANALYSIS OF THE INDUCED LOSS

WHEN PROFILE DRAG IS ABSENT

The expression for the efficiency of a section can be shown to be

$$\eta_i = \frac{\tan \phi'}{\tan \phi}$$

From figure 1, this expression can be revised to

$$\eta_i = \frac{V}{x\pi n D} \bigg/ \frac{V + w}{x\pi n D}$$

$$= \frac{1}{1 + \dfrac{w}{V}}$$

where $w = w_1 \sec \phi$ is an imaginary axial inflow velocity that, in the determination of induced loss and induced efficiency, is equivalent to both the actual axial inflow velocity w_a and the rotational inflow velocity w_r. Thus the total induced power loss at any section x is $\dfrac{dT_1}{dx} w$ and

$$\frac{dT_1}{dx} w = \frac{dT_1}{dx} w_a + \frac{dQ_1}{dx} w_r$$

From the fundamental Goldstein condition, $x \tan \phi$ = a constant, the following expressions can be derived:

$$x \tan \phi = \frac{V + w}{\pi n D} = \text{a constant}$$

Therefore w, the effective axial inflow velocity, and $\eta_i = \dfrac{1}{1 + \dfrac{w}{V}}$

are both constant along the blade.

The induced efficiency loss of any section can be expressed as

$$\Delta\eta_i = 1 - \frac{1}{1 + \frac{w}{V}}$$

$$= \frac{w}{V + w}$$

The part of this loss due to axial inflow is obviously

$$\Delta\eta_a = \frac{w_a}{V + w}$$

and the part due to slipstream rotation is

$$\Delta\eta_r = \frac{w_2}{V + w}$$

As ratios of the whole loss $\Delta\eta_i$ these expressions become

$$\frac{\Delta\eta_a}{\Delta\eta_i} = \frac{w_a}{w} = \cos^2\phi$$

and

$$\frac{\Delta\eta_r}{\Delta\eta_i} = \frac{w_2}{w} = \sin^2\phi$$

and, obviously,

$$\frac{\Delta\eta_a}{\Delta\eta_i} + \frac{\Delta\eta_r}{\Delta\eta_i} = 1$$

APPENDIX B

SOME IMPLICATIONS OF THE GOLDSTEIN THEORY

The inflow velocity for the idealized case, where the slipstream velocity is constant over the whole disk and where the propeller is lightly loaded and causes negligible slipstream contraction, may easily be calculated from basic formulas as follows:

Force = mass flow × change in velocity

For an annular element of width dr at radius r, this relation may be expressed as

$$2\pi r\ \sigma\ dr\ C_R \frac{\rho}{2} W^2 = \rho\ 2\pi r\ dr\ W \sin\phi\ 2w_1$$

which simplifies to

$$w_1 = \frac{\sigma C_R W}{4 \sin \phi} \tag{B-1}$$

where C_R is the vector sum of C_L and C_D as shown in figure 1.

The slipstream velocity in any practical case is not constant over the propeller disk but consists of peaks of high velocity ahead of and behind each blade and valleys of low velocity between the blades. The peaks ahead of and behind each blade vary in magnitude with the radius, the number of blades, and the angle ϕ. The variation of the magnitude of the peaks with these factors was evaluated by Goldstein (reference 5) for a few simple cases and was later expanded by Lock and others to cover a wider range of cases, that is, for two-, three-, and four-blade propellers. It is shown in reference 2 that peak inflow velocity may be obtained by the use of a factor K in equation (B-1);

thus,

$$w_1 = \frac{\sigma C_R W}{4K \sin \phi} \tag{B-2}$$

where K (called the Goldstein factor) varies with the B, x, and ϕ. Plots of K against $\sin \phi$ with x as a parameter given in figures 2, 3, and 4 and for two-, three-, and four-blade propellers were reproduced from reference 2.

For the case in which profile drag is assumed to be zero, equation (B-2) becomes

$$w_1 = \frac{\sigma C_L W}{4K \sin \phi} \tag{B-3}$$

and

$$w = \frac{w_1}{\cos \phi} = \frac{\sigma C_L W}{4K \sin \phi \cos \phi} = \frac{bB\, C_L W}{8K \cdot \pi x R \sin \phi \cos \phi} \tag{B-4}$$

As

$$W \approx W_0 = \sqrt{V^2 + (Sx)^2}$$

$$bC_L = \frac{4wK \sin \phi \cos \phi\, \pi Dx}{B W_0} \tag{B-5}$$

In a particular design, B, n, D, S, and V will be known and, for optimum loading, w will be a constant. The quantities K, ϕ, W_0, and thus bC_L, will therefore become functions of x.

As ϕ differs little from ϕ', it may be assumed, as an approximation, that

$$h \pi Dx/W_0 \approx \cos \phi$$

and so equation (B-5) may be written

$$bC_L \approx \frac{4wK \sin \phi \cos^2 \phi}{Bn} \tag{B-6}$$

which, for a particular design with optimum loading, becomes

$$bC_L \approx kK \cdot \sin \phi \cos^2 \phi \tag{B-7}$$

Equation (B-7) is the one used in section I of this report.

APPENDIX C

A DISCUSSION OF BLADE NUMBER

The commonly used term "tip loss" is a rather inexact name to apply to a loss that, although greater at the tips, extends over the whole blade, the case being parallel to that of the induced drag of a tapered wing. There would be no tip loss and the Goldstein factor (see appendix B) would be 1 if the the propeller (1) had an infinite number of blades, (2) turned at an infinite speed, or (3) had an infinite diameter. Corresponding conditions, that is, (1) infinite multiplane, (2) infinite airspeed, or (3) infinite span, eliminate the induced drag of a wing.

Another aspect of the so-called tip loss that conveys a somewhat clearer picture is: The slipstream velocity would be constant over the whole slipstream cross section both in front of and behind a propeller with an infinite number of blades. If the number of blades is reduced and becomes finite, variations of velocity in the slipstream occur and the efficiency drops from the ideal value for an infinite number of blades. The loss can be explained by simple axial momentum theory although the rotational velocities neglected in such theory play an important part in the loss. According to simple axial momentum theory, the loss in efficiency results from the fact that a given thrust, represented by the change in momentum of the air flowing through the propeller disk, is accompanied by a change in kinetic energy in the slipstream, which is greater than the work done (TV). This loss will be a minimum for a given thrust when the velocity is uniform over any cross section parallel to the propeller plane.

A simplified analogy follows: Two masses m_1 and m_2 moving in the same direction at velocities v_1 and v_2 have a total momentum $M = m_1 v_1 + m_2 v_2$. It can easily be proved that the kinetic energy, $K_1 = \frac{1}{2} m_1 v_1^2 + \frac{1}{2} m_2 v_2^2$, will be a minimum for a given M when the velocities v_1 and v_2 are equal.

The loss in efficiency (for a constant thrust) will clearly become increasingly greater as the variations (or periodicity) of the slipstream become greater, and the periodicity obviously increases as the number of blades decreases, the greatest periodicity occurring for a one-blade propeller.

Assume, for example, a hypothetical eight-blade propeller turning at a constant rotational speed. If one blade is removed, the thrust is reduced by approximately 12.5 percent. The efficiency rises as a result of the lower disk loading but the rise is offset a small amount by the loss accompanying the increased periodicity of the flow in the slipstream. If one after another of the blades is removed, the induced efficiency rises but, for each additional blade removed, the offset resulting from increased periodicity becomes greater until a number of blades is reached where the removal of one more blade decreases rather than increases the efficiency. The loss caused by the increased periodicity resulting from the removal of the blade more than offsets the gain in efficiency resulting from the lower thrust loading on the propeller disk. The critical number of blades at which this condition is reached depends on the operating conditions. The tests reported in reference 6 on 10-foot propellers seem to indicate that the critical number of blades for the conditions existing in those tests was three. The efficiency of the three-blade propeller was the same as, if not a little higher than, the efficiency of the two-blade propeller. The efficiency of a one-blade propeller, had it been tested, would probably have been somewhat lower than the efficiency of the two-blade propeller.

APPENDIX D

CRITERIONS FOR DIAMETER SELECTION

The selection of the optimum diameter is another problem related to the design of an optimum propeller. Two conflicting factors must be balanced in order to achieve the propeller of maximum efficiency. These factors are the profile-drag loss and the induced loss. The profile-drag loss increases and the induced loss decreases with increases in the propeller diameter if the tip speed is held constant.

In the determination of the relation between optimum diameter and the two types of propeller loss, it will be convenient to assume that P, $T\left(=\frac{\eta P}{V}\right)$, $\pi n D$ (tip speed), ρ, and V are essentially constant and that, for any station x, ρ, b, ϕ, ϕ', and C_{D_0} are also constant. Then dT_1/dx for any particular station x will be constant and C_L will be an inverse function of R; that is, $C_L = k/R$.

On the basis of the previously stated assumptions, the value of w as given in appendix B may be expressed as

$$w = \frac{bB \; C_L \; W}{8K \; \pi x R \; \sin \phi \; \cos \phi} = \frac{k_1}{R^2}$$

Equation (9) and appendix A yield the following expressions for the differential profile-drag and induced power losses:

$$\frac{dP_{D_0}}{dx} = RB \; bC_{D_0} \; \frac{\rho}{2} \; \frac{V^3}{\sin^3\phi'} = k_2 R$$

$$\frac{dP_1}{dx} = \frac{dT_1}{dx} \; w = \frac{k_3}{R^2}$$

As the differential power losses are functions only of R, then the over-all losses will also be functions only of R. Thus

$$P_{D_0} = k_4 R$$

$$P_1 = \frac{k_5}{R^2}$$

The total loss, P_L, will be

$$P_L = P_{D_o} + P_1 = k_4 R + \frac{k_5}{R^2}$$

If the equation is differentiated and put equal to zero,

$$\frac{dP_L}{dR} = k_4 - \frac{2k_5}{R^3} = \frac{P_{D_o}}{R} - \frac{2P_1}{R} = 0$$

Therefore, under the conditions assumed, the optimum diameter for the optimum propeller will be one that will cause $P_{D_o} = 2P_1$; that is, it will be a propeller for which the profile-drag losses are twice as great as the induced losses.

In this analysis, b, for a given value of x, and tip speed were held constant and independent of variations in R. If geometric similarity had been assumed, then $b \propto R$ and $C_L \propto \frac{1}{b}\frac{1}{R}$ or $\frac{1}{R^2}$. The analysis would then have produced the result $P_{D_o} = P_1$.

If the tip speed had been permitted to vary directly with R (that is, $n = $ constant), another result might have been obtained. The equations for this case are more complex, however, and their solution was not attempted.

It may be of interest to note that, in the case of the optimum propeller designed in an earlier section of this report, the power losses, expressed as percentages of the total power input, were

$$P_{D_o} = 3.07$$
$$P_1 = 4.00$$

These values suggest that a lower total loss, P_L, might have been obtained if the diameter had been larger.

REFERENCES

1. Lock, C. N. H., and Bateman, H.: Wind Tunnel Tests of High Pitch Airscrews. Part II. Variations of Blade Width and Blade Section. R. & M. No. 1729, British A.R.C., 1936.

2. Lock, C. N. H., and Yeatman, D.: Tables for Use in an Improved Method of Airscrew Strip Theory Calculation. R. & M. No. 1674, British A.R.C., 1935.

3. Stack, John: Tests of Airfoils Designed to Delay the Compressibility Burble. NACA Rep. No. 763, 1943.

4. Stickle, George W.: Measurement of the Differential and Total Thrust and Torque of Six Full-Scale Adjustable-Pitch Propellers. NACA Rep. No. 421, 1932.

5. Goldstein, Sydney: On the Vortex Theory of Screw Propellers. Proc. Roy. Soc. (London), ser. A, vol. 123, no. 792, April 6, 1929, pp. 440-465.

6. Hartman, Edwin P., and Biermann, David: The Aerodynamic Characteristics of Full-Scale Propellers Having 2, 3, and 4 Blades of Clark Y and R.A.F. 6 Airfoil Sections. NACA Rep. No. 640, 1938.

TABLE II

COMPUTATIONS FOR OPTIMUM BLADE LOADING

AND FIXED BLADE CHARACTERISTICS

x	$\tan\phi$	ϕ (deg)	$\sin\phi$	$\cos\phi$	K	$\cos^2\phi$	$(K\sin\phi)$ $\times(\cos^2\phi)$	$\dfrac{bC_L}{bC_{L_{x=0.7}}}$	bC_L (in.)	$\tan\phi'$	ϕ' (deg)	α_1 (deg)	xS (fps)	$W=\dfrac{xS}{\cos\phi'}$ (fps)	M
0.30	1.690	59.4	0.861	0.509	1.036	0.259	0.231	0.910	2.84	1.620	58.3	1.1	271	516	0.464
.45	1.125	48.4	.748	.664	.864	.441	.285	1.122	3.50	1.080	47.2	1.2	406	599	.536
.60	.845	40.2	.646	.764	.744	.584	.280	1.102	3.44	.811	39.1	1.1	542	699	.626
.70	.725	35.9	.586	.810	.661	.656	.254	1.000	3.12	.695	34.8	1.1	633	770	.691
.80	.634	32.4	.536	.844	.554	.713	.211	.831	2.59	.608	31.3	1.1	723	845	.757
.90	.563	29.4	.491	.871	.403	.759	.150	.591	1.84	.541	28.4	1.0	813	925	.830
.95	.533	28.1	.471	.882	.290	.777	.106	.418	1.30	.512	27.1	1.0	858	966	.866

TABLE III

SAMPLE COMPUTATIONS

x \\ h/b	0.30	0.45	0.60	0.70	0.80	0.90	0.95
$b = h/\frac{h}{b}$, in.							
0.06	41.70	21.30	15.32	12.32	9.68	7.16	6.00
.09	27.8	14.20	10.22	8.22	6.45	4.78	4.00
.12	20.9	10.68	7.66	6.16	4.84	3.58	3.00
.15	16.7	8.54	6.13	4.94	3.87	2.86	2.40
$c_L = bc_L/b$							
0.06	0.0681	0.164	0.224	0.253	0.268	0.257	0.217
.09	.1022	.246	.335	.382	.402	.385	.326
.12	.136	.385	.449	.510	.535	.515	.434
.15	.170	.410	.561	.636	.670	.645	.533
c_{D_0} from figure 14							
0.06	0.00355	0.00398	0.00420	0.00420	0.00397	0.00423	0.00420
.09	.00390	.00465	.00497	.00520	.00536	.00522	.00490
.12	.00490	.00665	.00715	.00765	.00780	.00768	.00700
.15	.00725	.00930	.01005	.01068	.01095	.01075	.00985
bc_{D_0}, in.							
0.06	0.1478	0.0848	0.0644	0.0518	0.0384	0.0303	0.0252
.09	.1085	.0660	.0508	.0427	.0346	.0249	.0196
.12	.1025	.0710	.0547	.0471	.0378	.0274	.0210
.15	.121	.0794	.0616	.0527	.0423	.0308	.0236
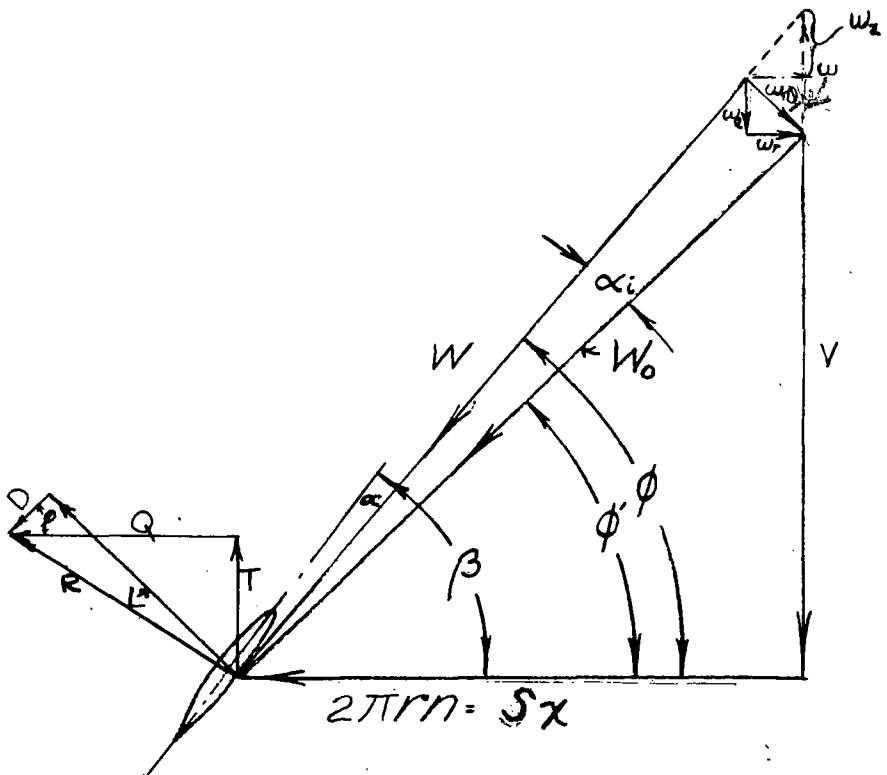
Figure 1.- Quantities defined at blade element.
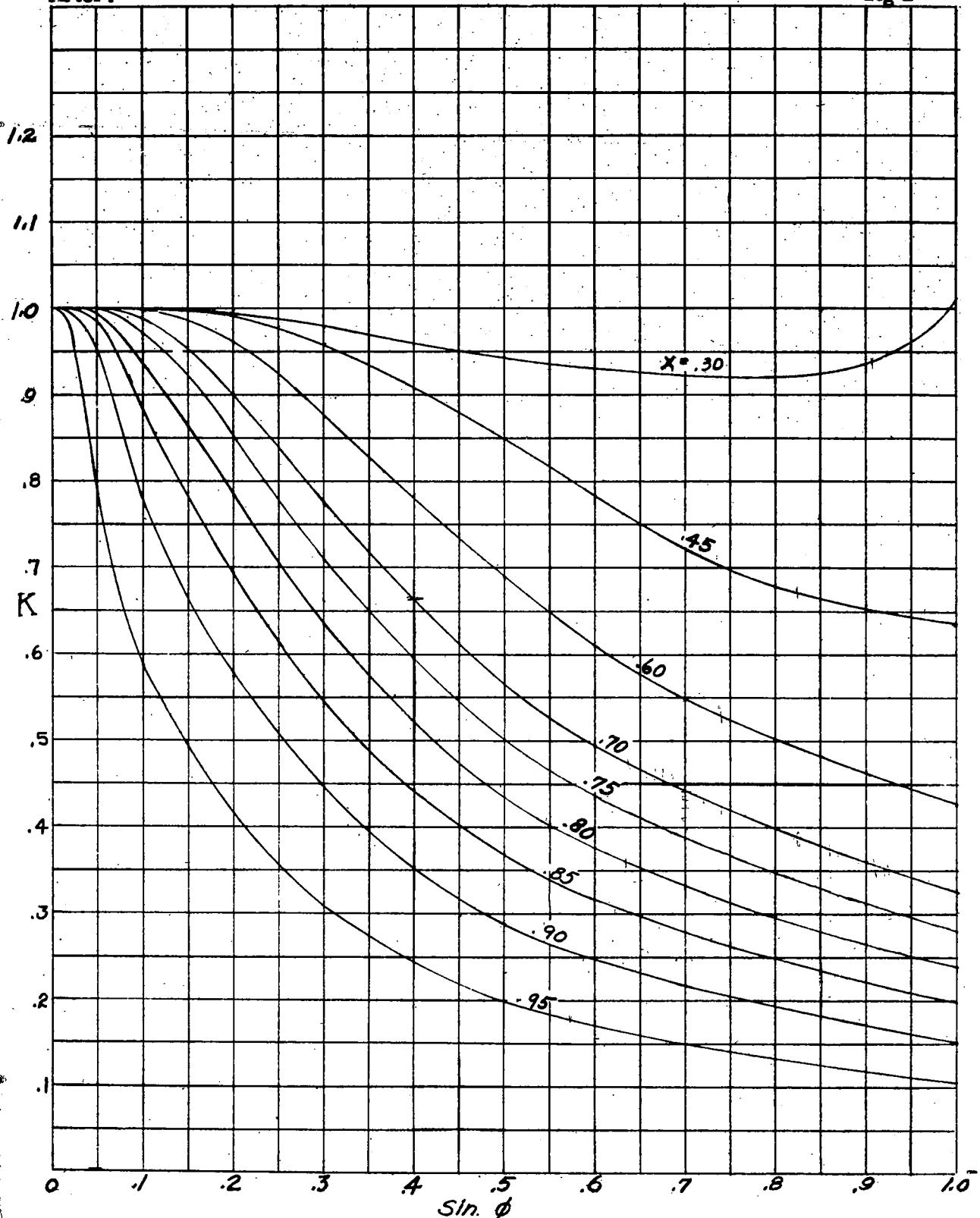
Figure 2.— Goldstein factors for two-blade propellers. Reproduced from reference 2.
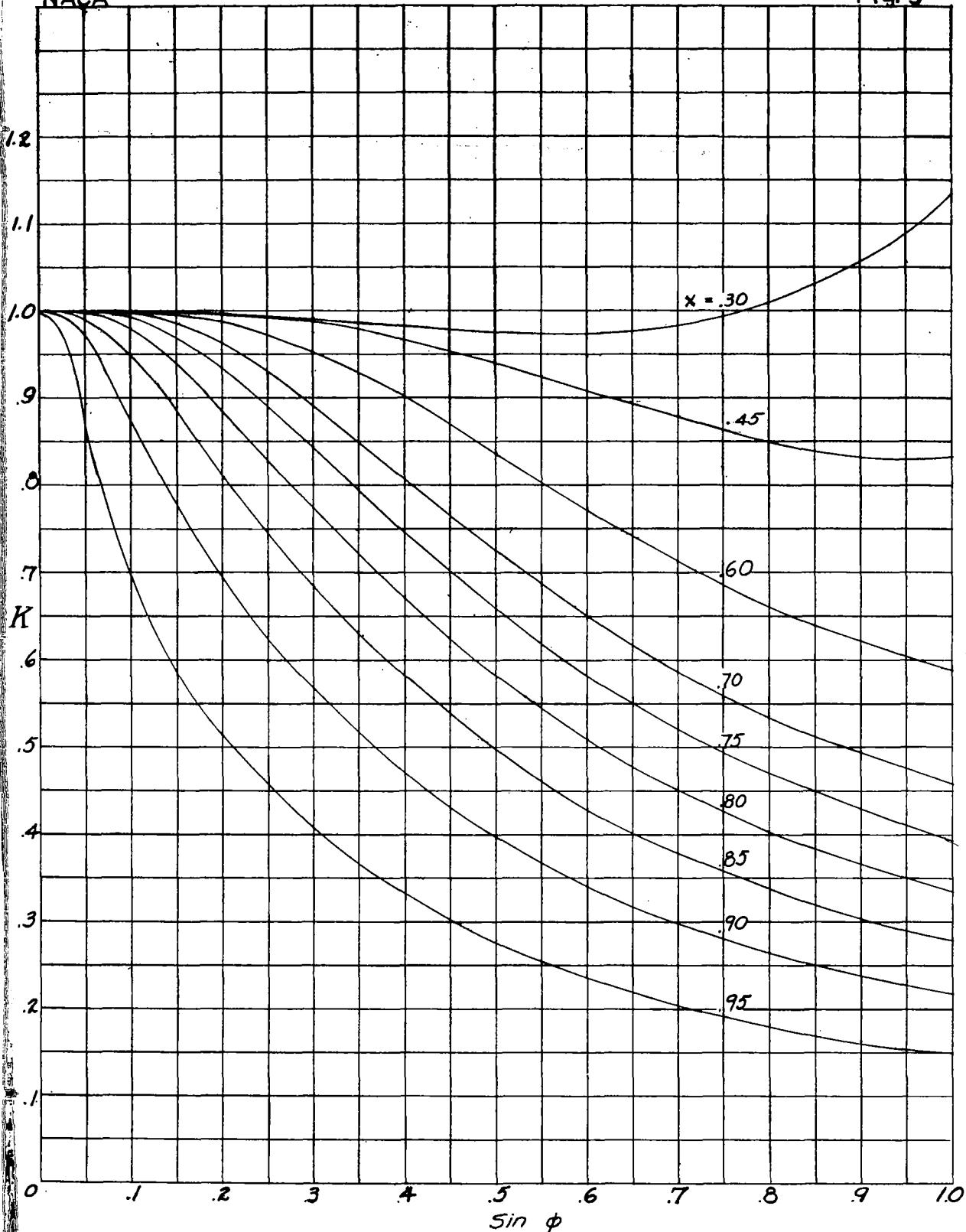
Figure 3.- Goldstein factors for three-blade propellers.
Reproduced from reference 2.
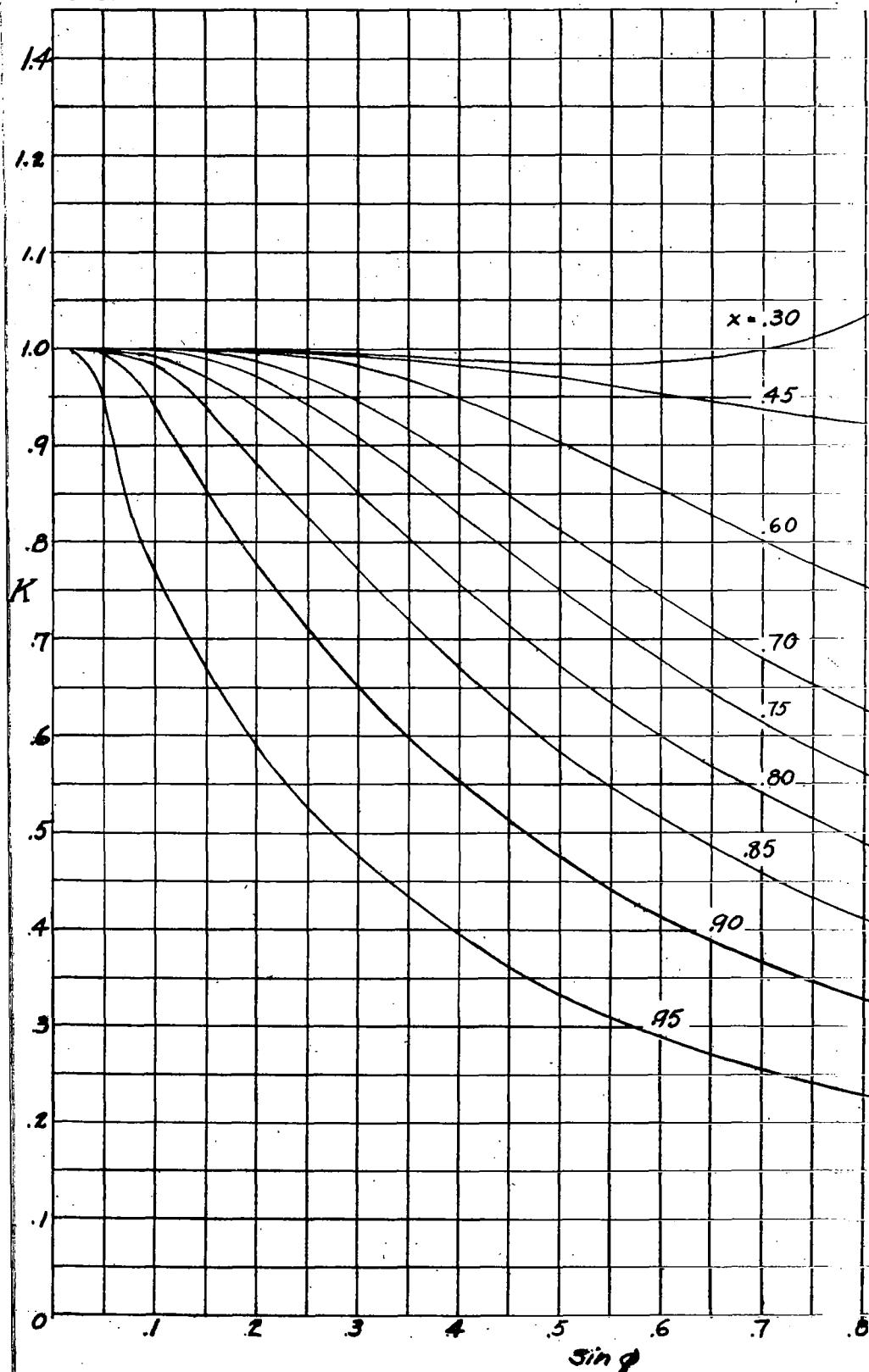
Figure 4.- Goldstein factors for four-blade propeller.
Reproduced from reference 2.
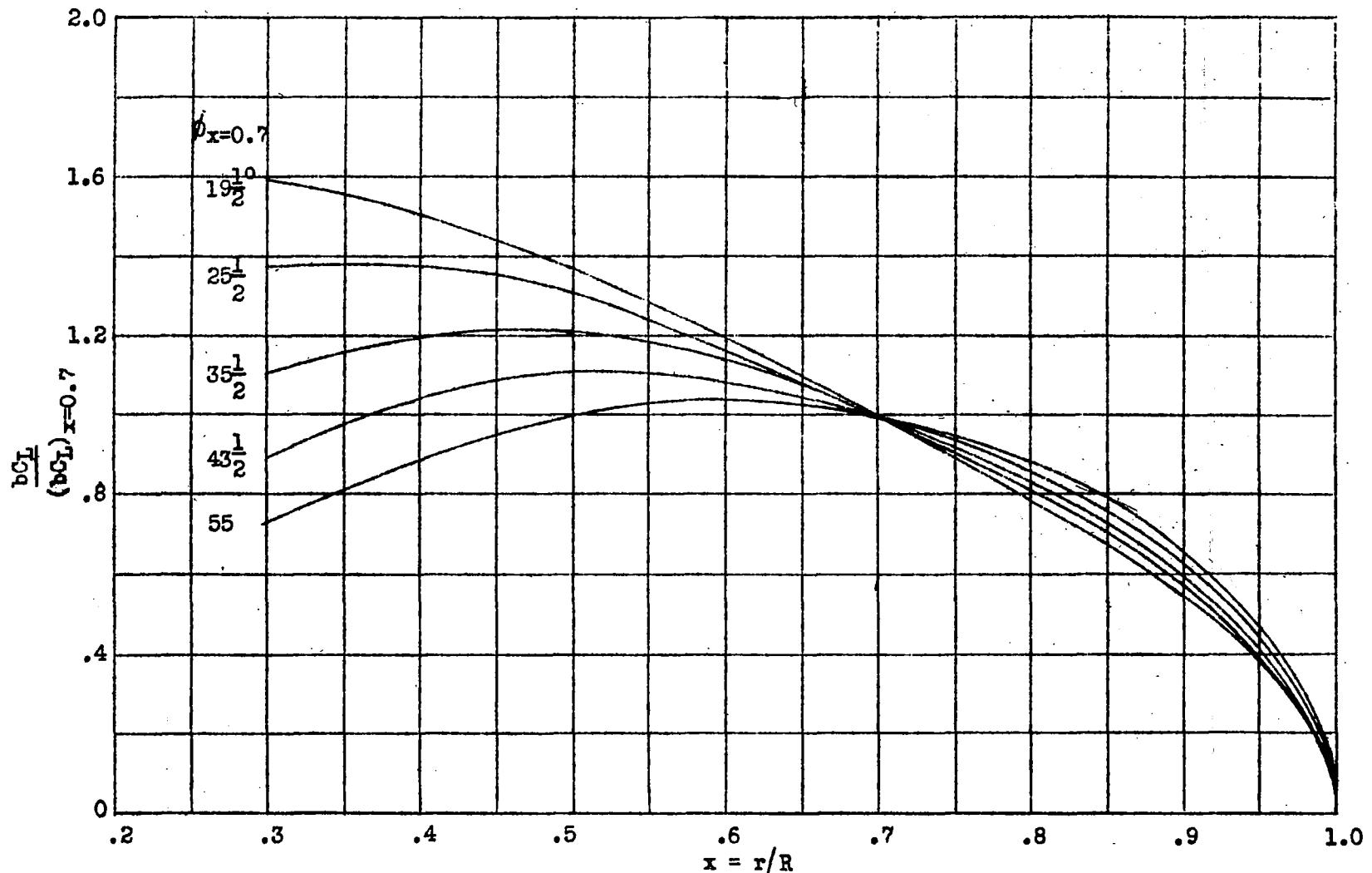
Figure 5.- Family of Betz loadings for two-blade propellers.

Fig. 5

$\frac{bC_L}{(bC_L)_{x=0.7}}$

$\phi_{x=0.7}$

$19\frac{1}{2}^{\circ}$

$25\frac{1}{2}$

$35\frac{1}{2}$

$43\frac{1}{2}$

55

$x = r/R$
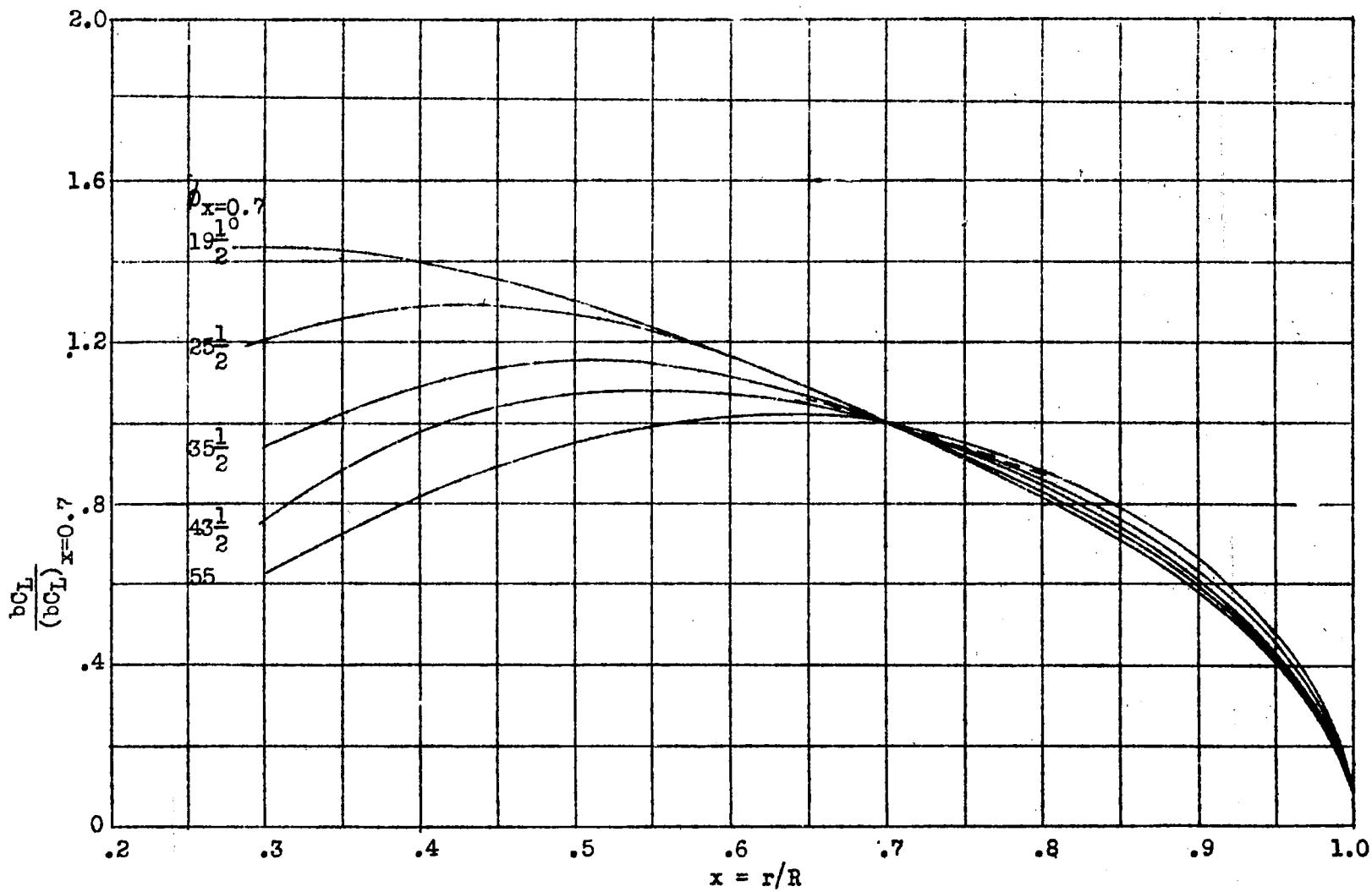
Figure 6.- Family of Betz loadings for three-blade propellers.

Fig. 6
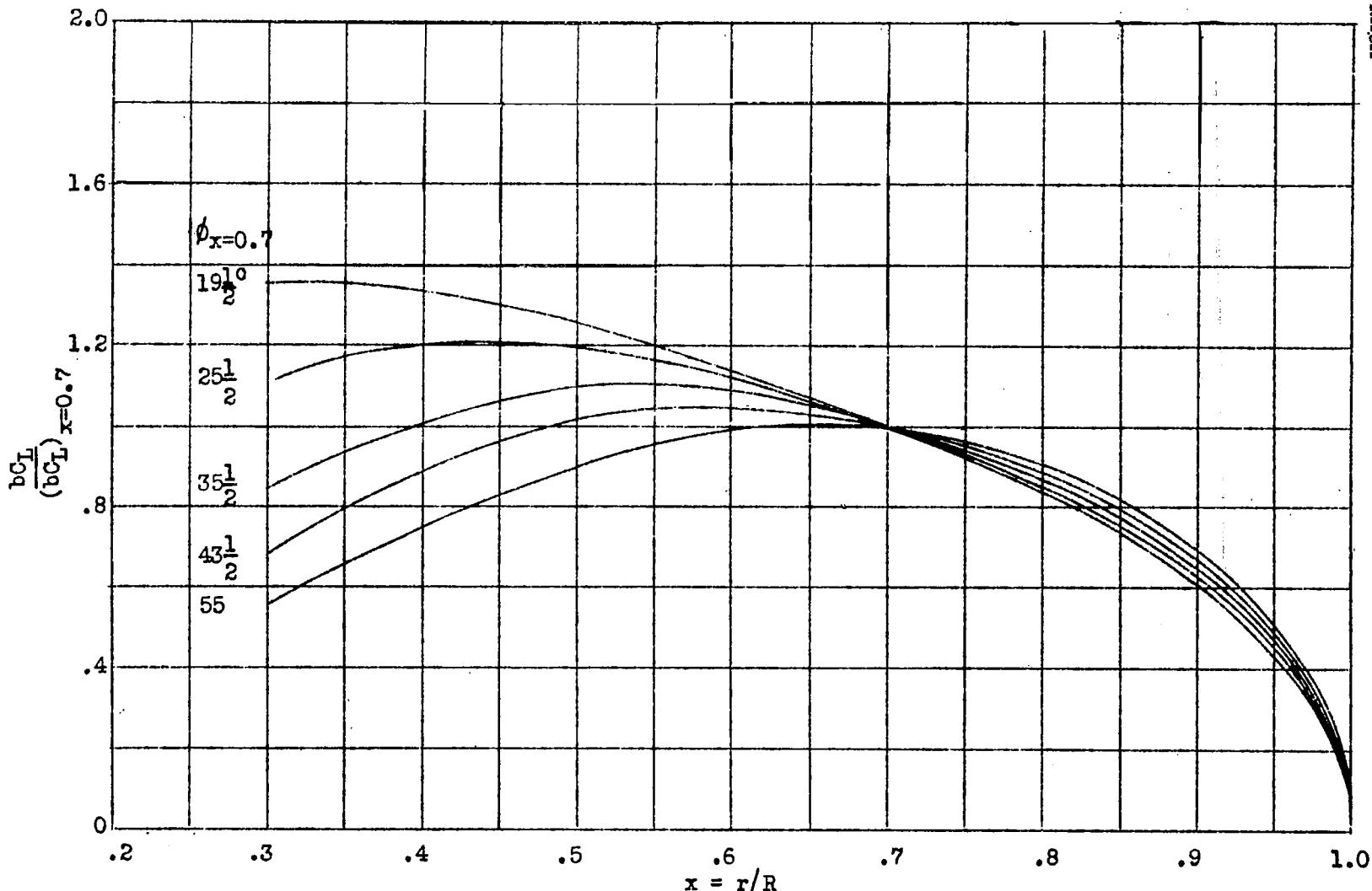
Figure 7.- Family of Betz loadings for four-blade propellers.

Fig. 7
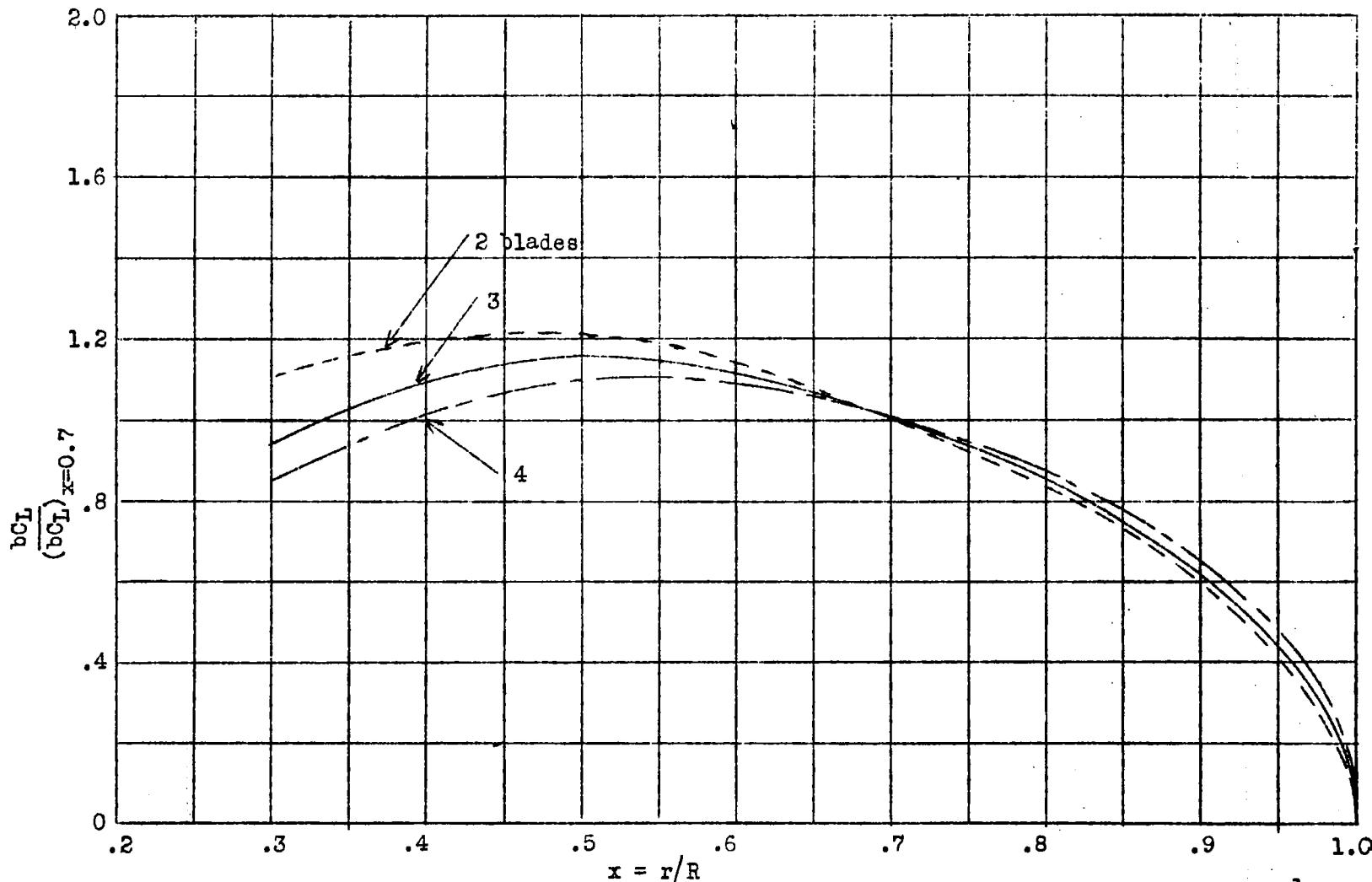
Figure 8.- Comparison of Betz loadings for two, three, and four-blade propellers. $\phi_{x=0.7} = 35\frac{1}{2}°$

Fig. 8
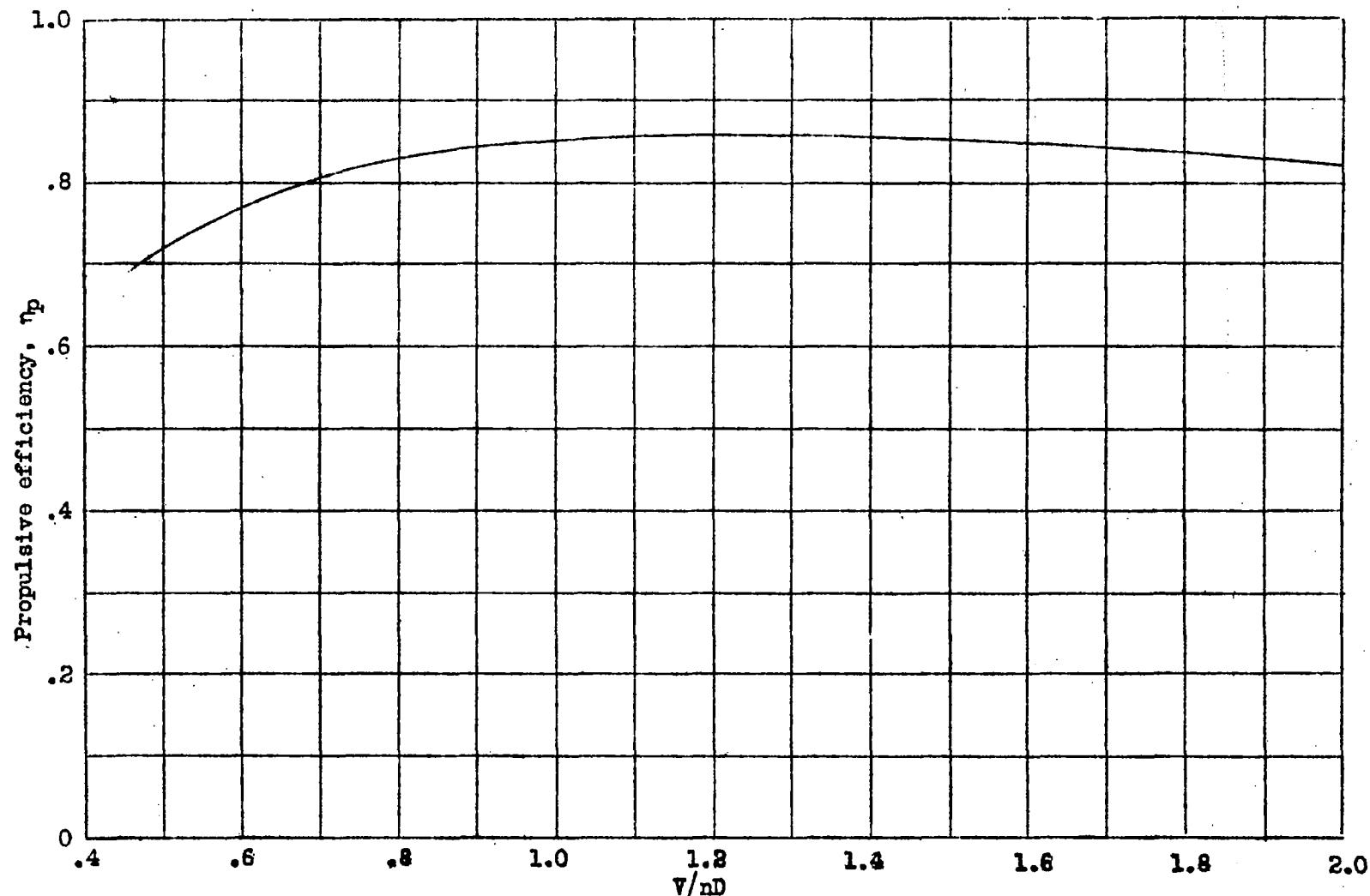
Figure 9.- Efficiency-curve envelope, taken from reference 6, for three-bladed 5868-9 propeller with Clark Y sections.

Fig. 9
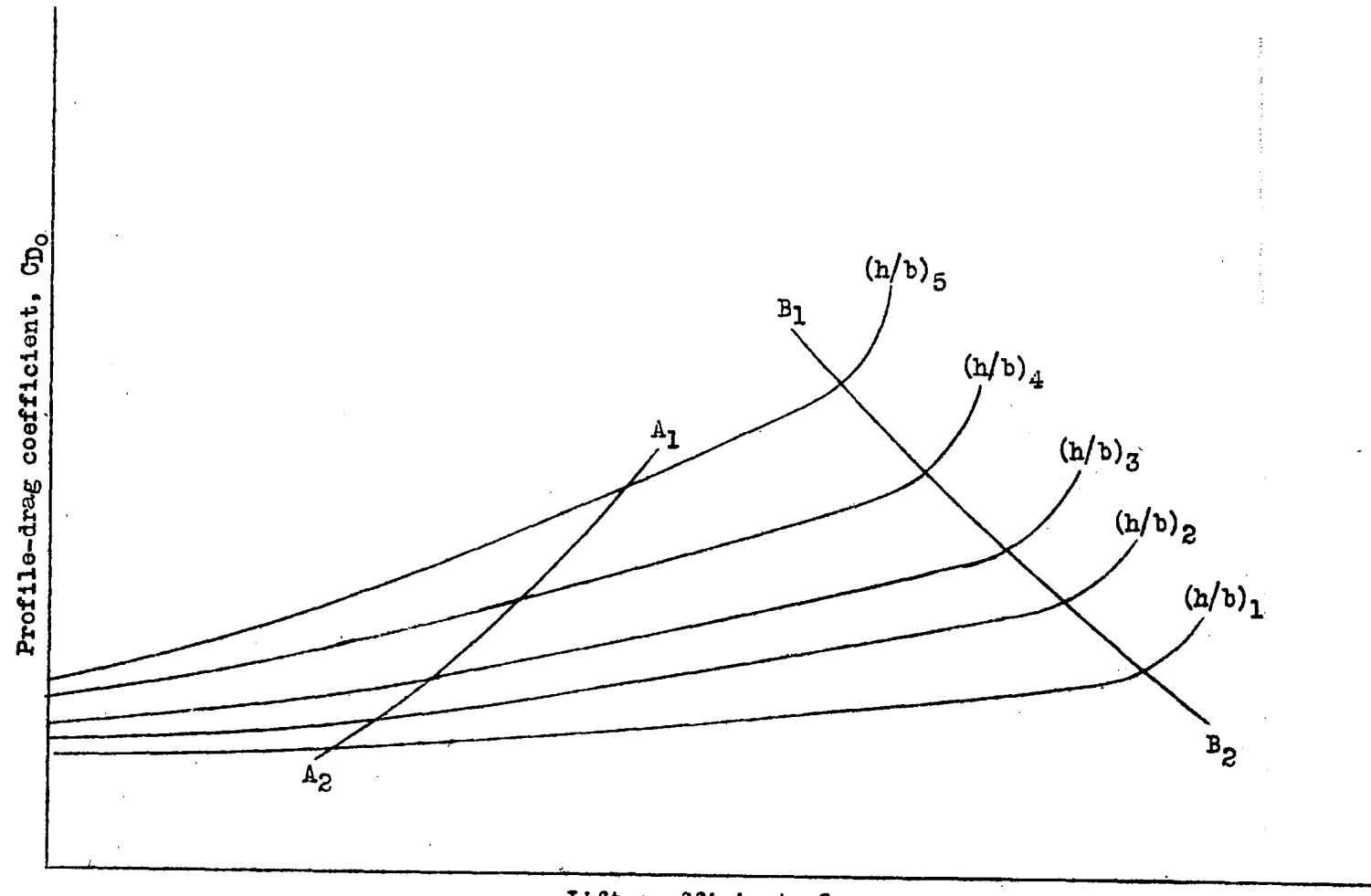
Figure 10.- Envelope drag curves for family at M = K.

Fig. 10
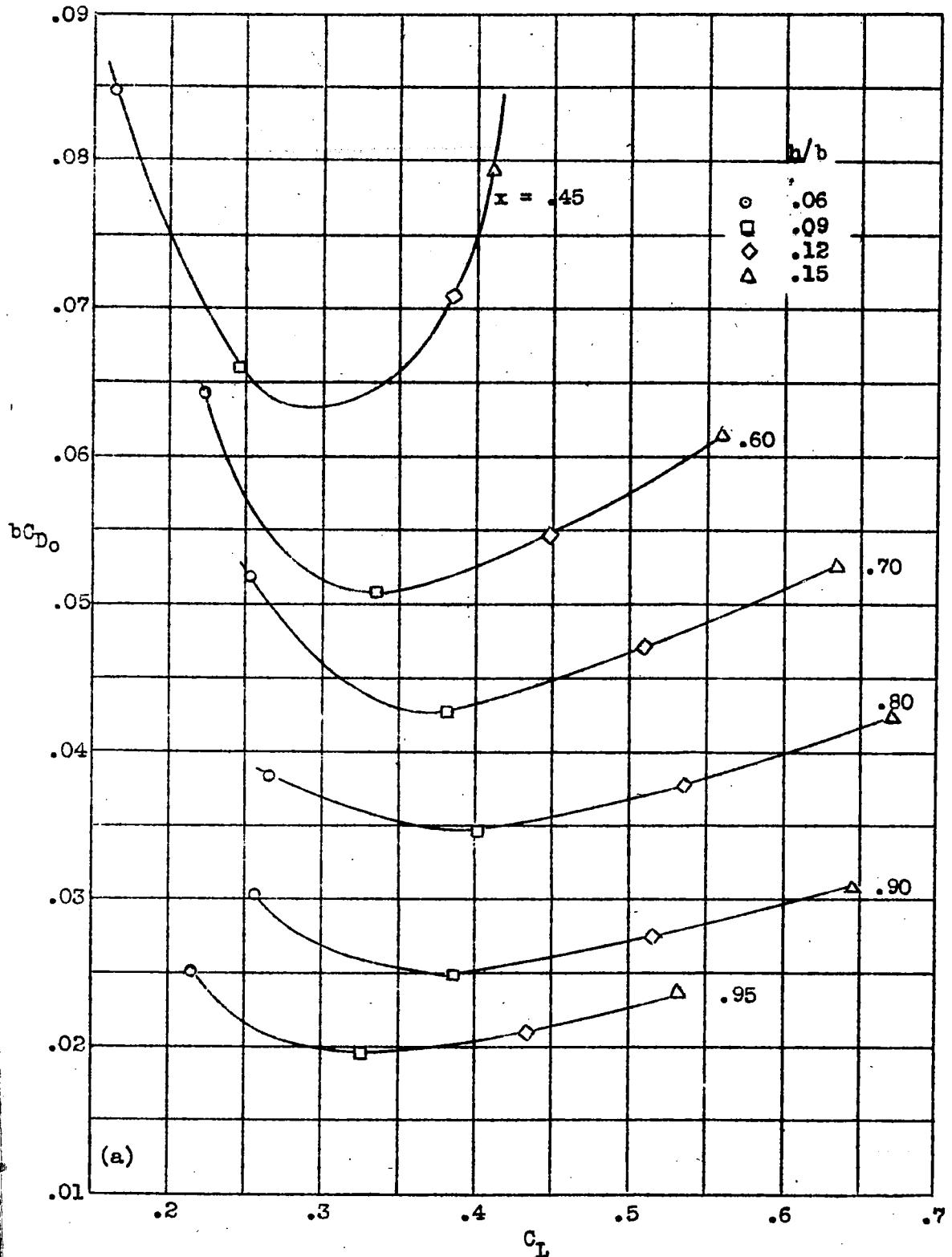
Figure 11(a,b).- Plots of bC_{D_o} against C_L for each station analyzed.
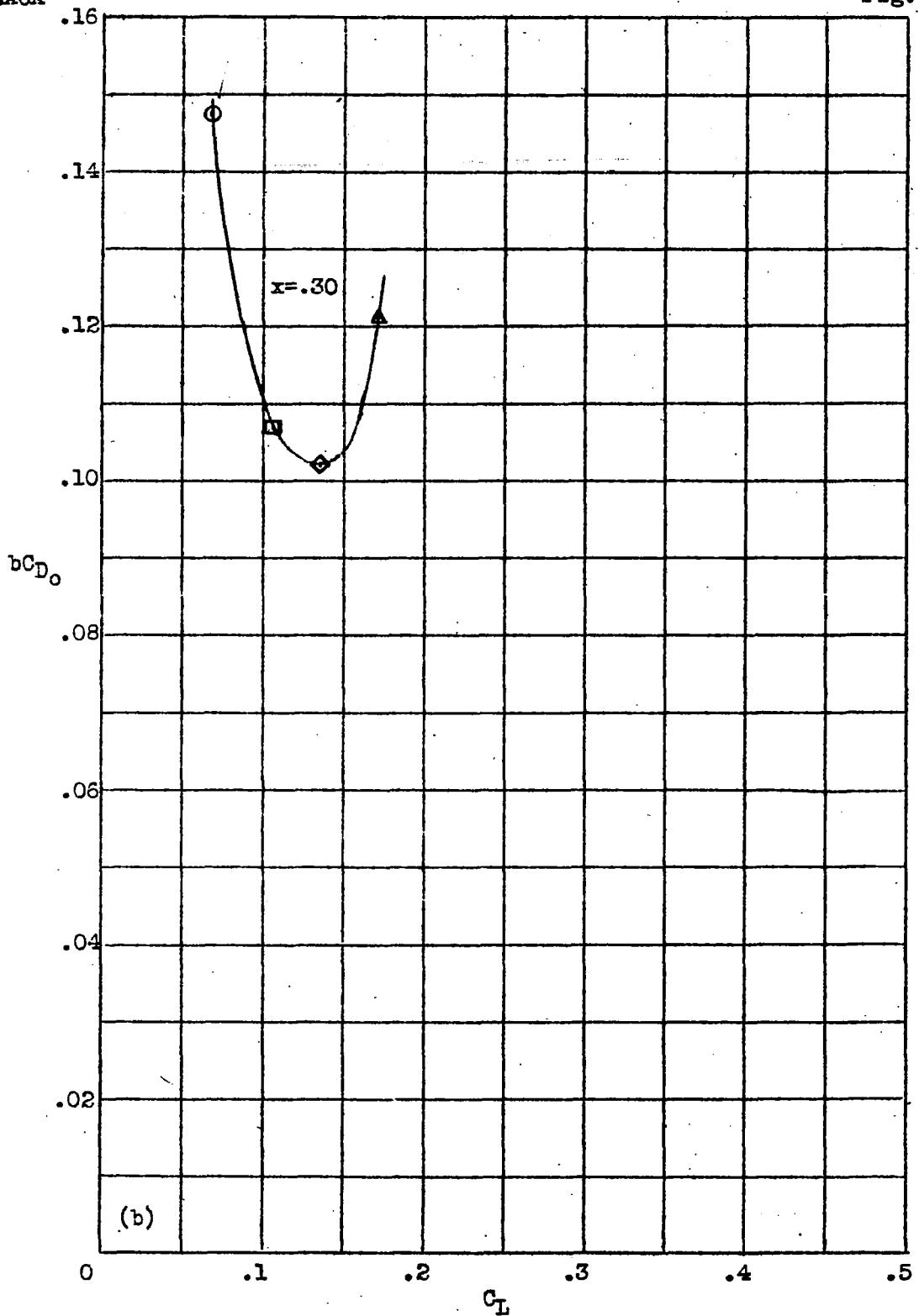
Figure 11.- Concluded
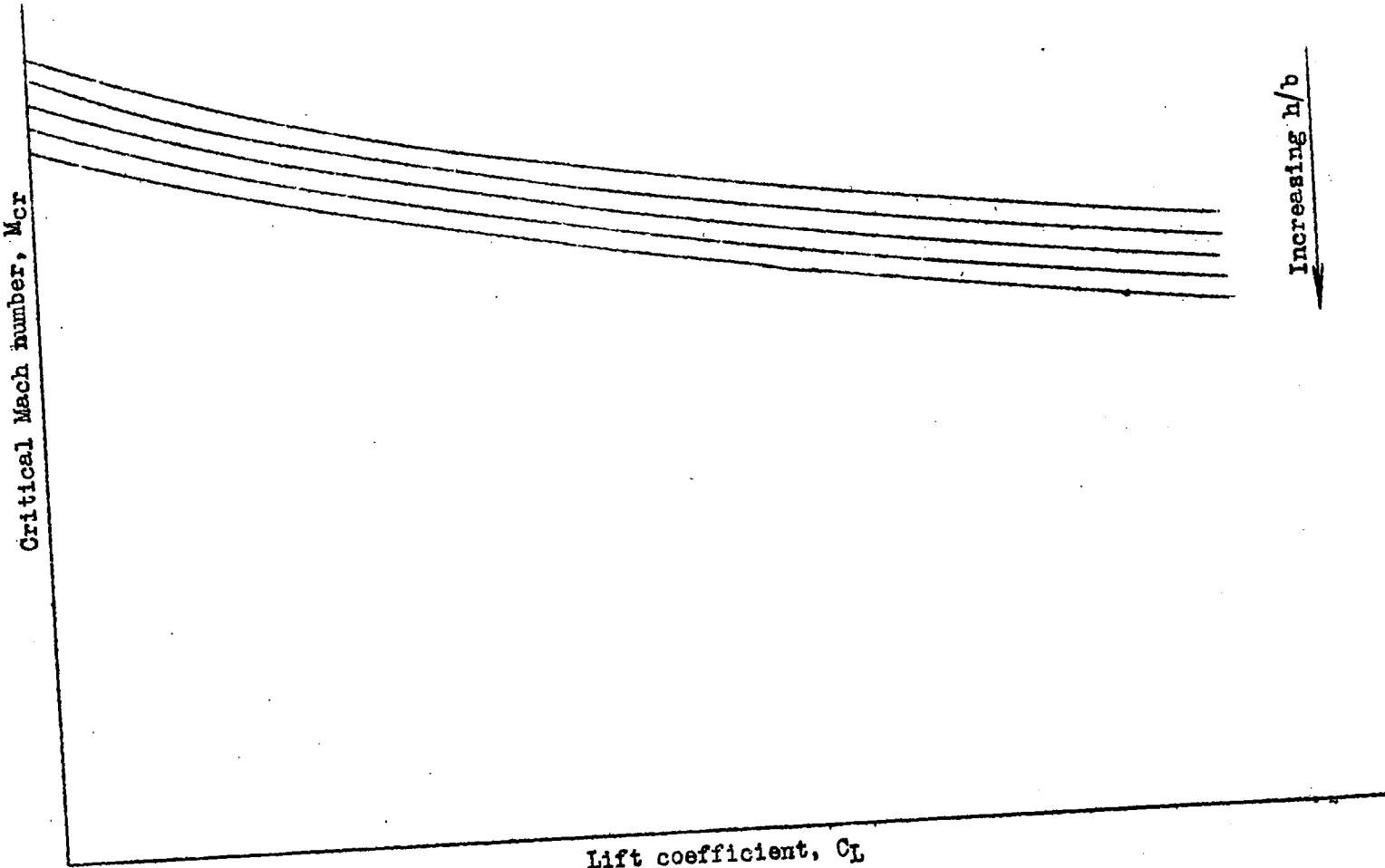
Figure 12.- Curves of critical Mach number M_{cr} for various thickness ratios.

Fig. 12
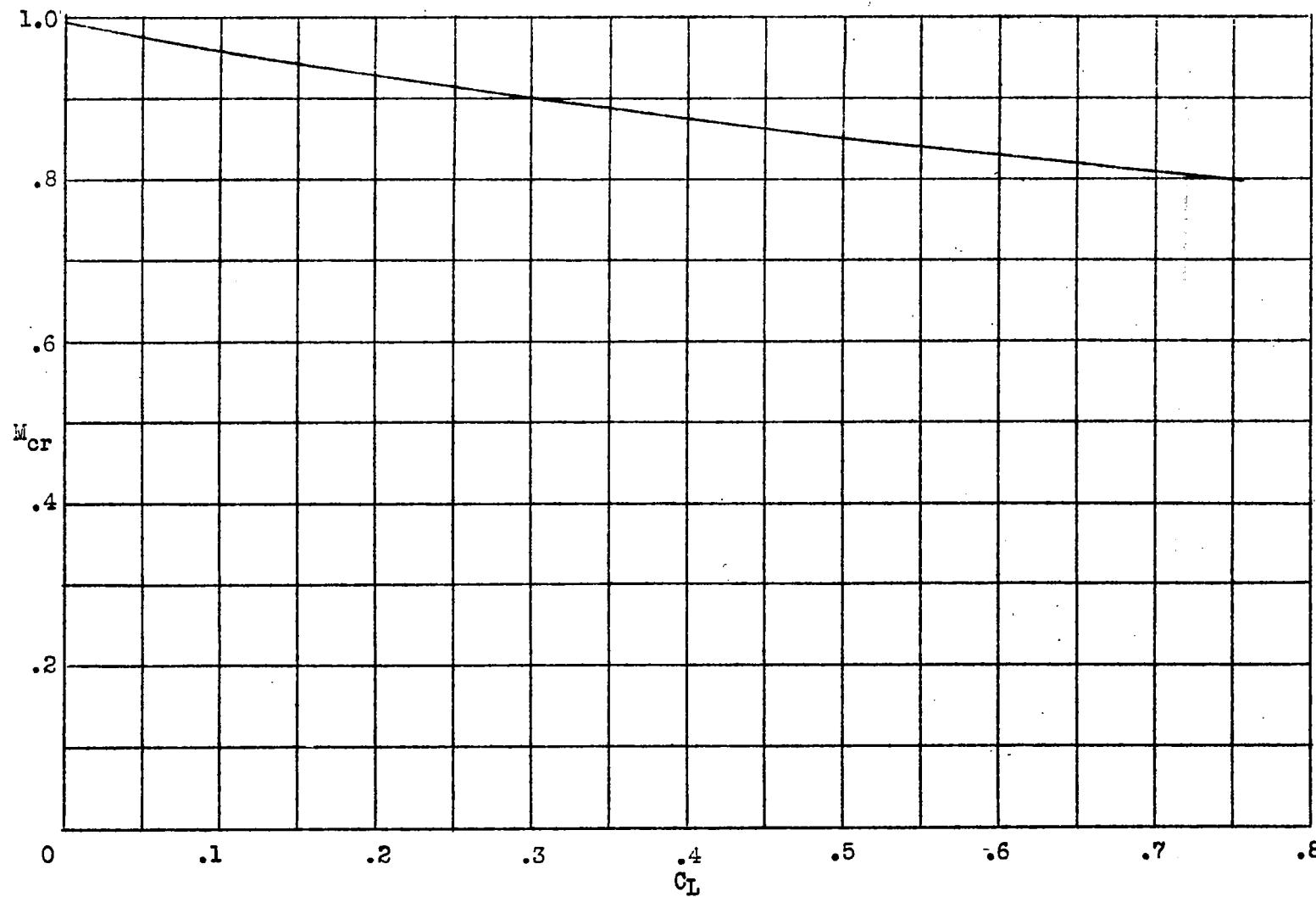
Figure 13.- Extrapolated curve of critical speed for propeller tip with 6-percent high-speed section from data in references 3 and 4.

Fig. 13
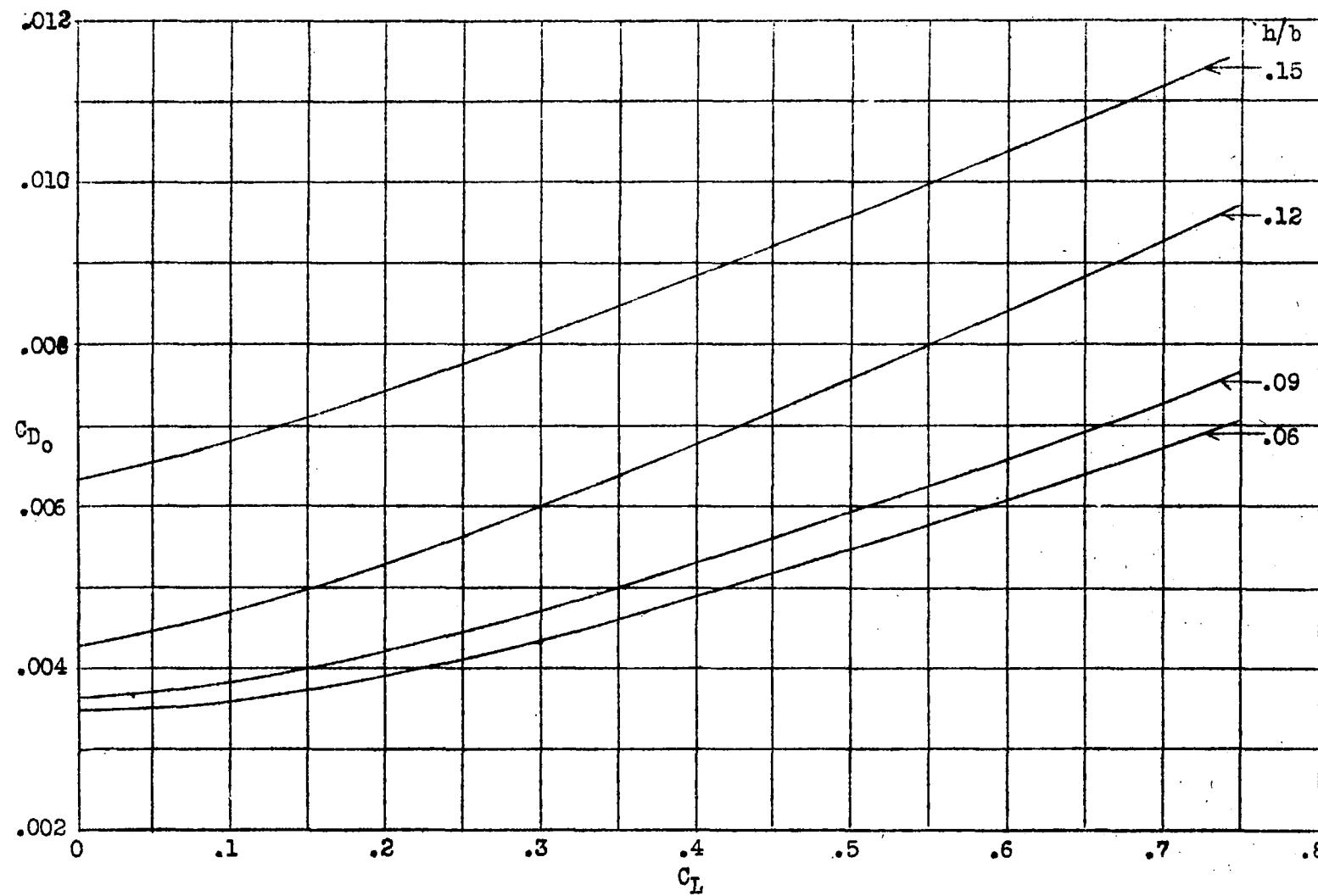
Figure 14.- Envelope drag curves for 16-Series Sections. M = 0.60.

Fig. 14
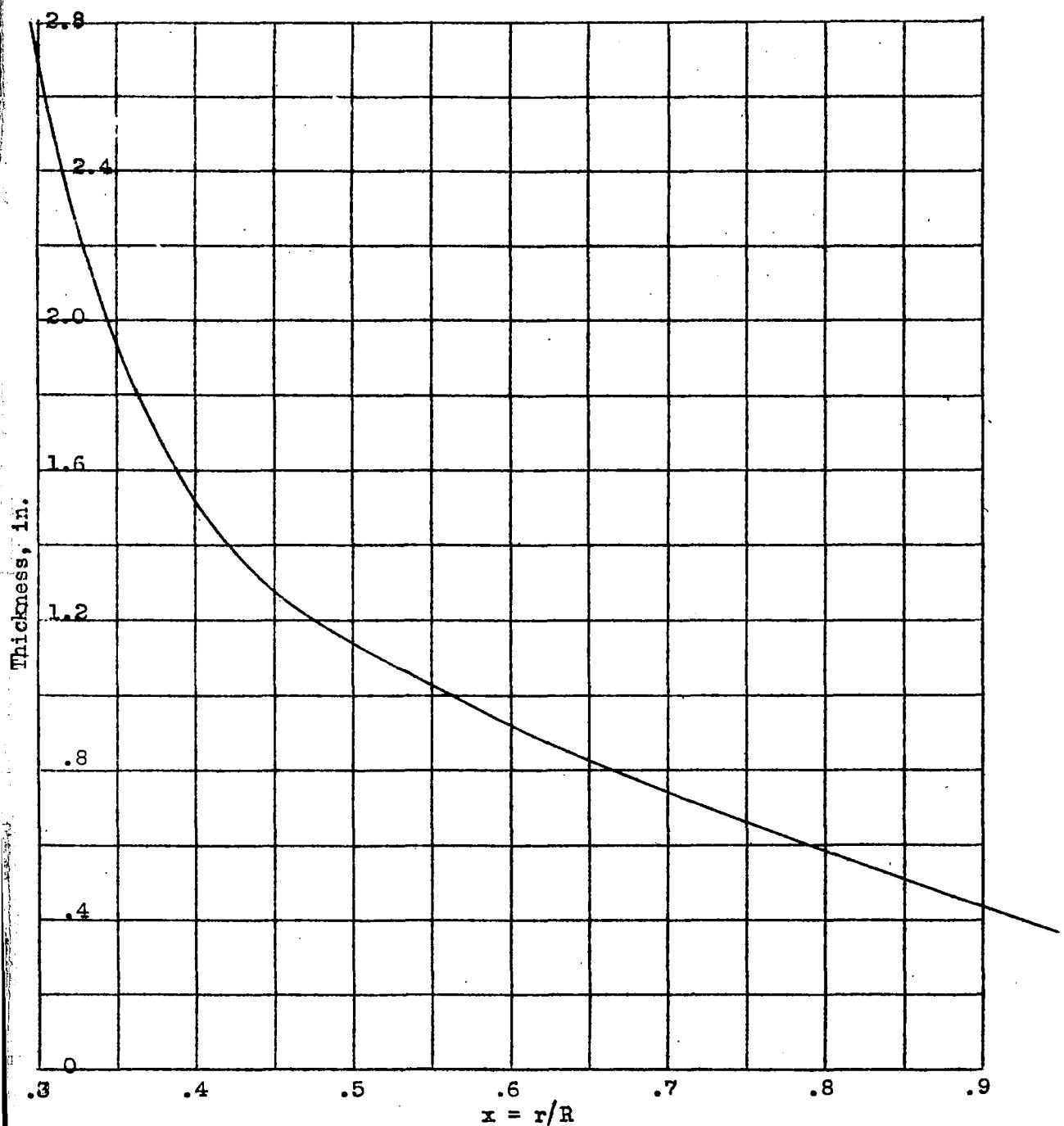
Figure 15.- Assumed radial thickness distribution.
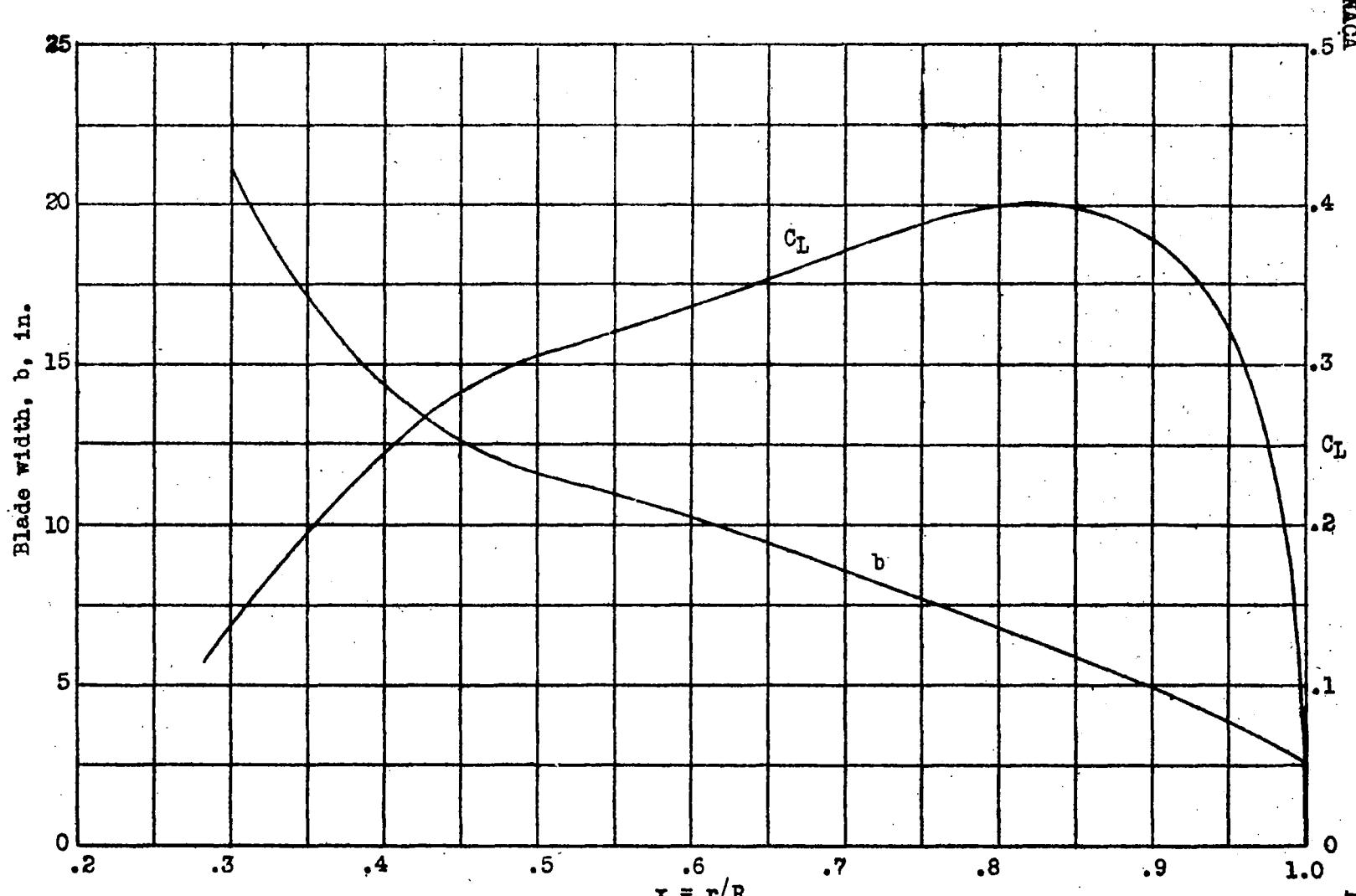
Figure 16.- Distribution of b and C_L for best blade shape designed for high speed.

Fig. 16
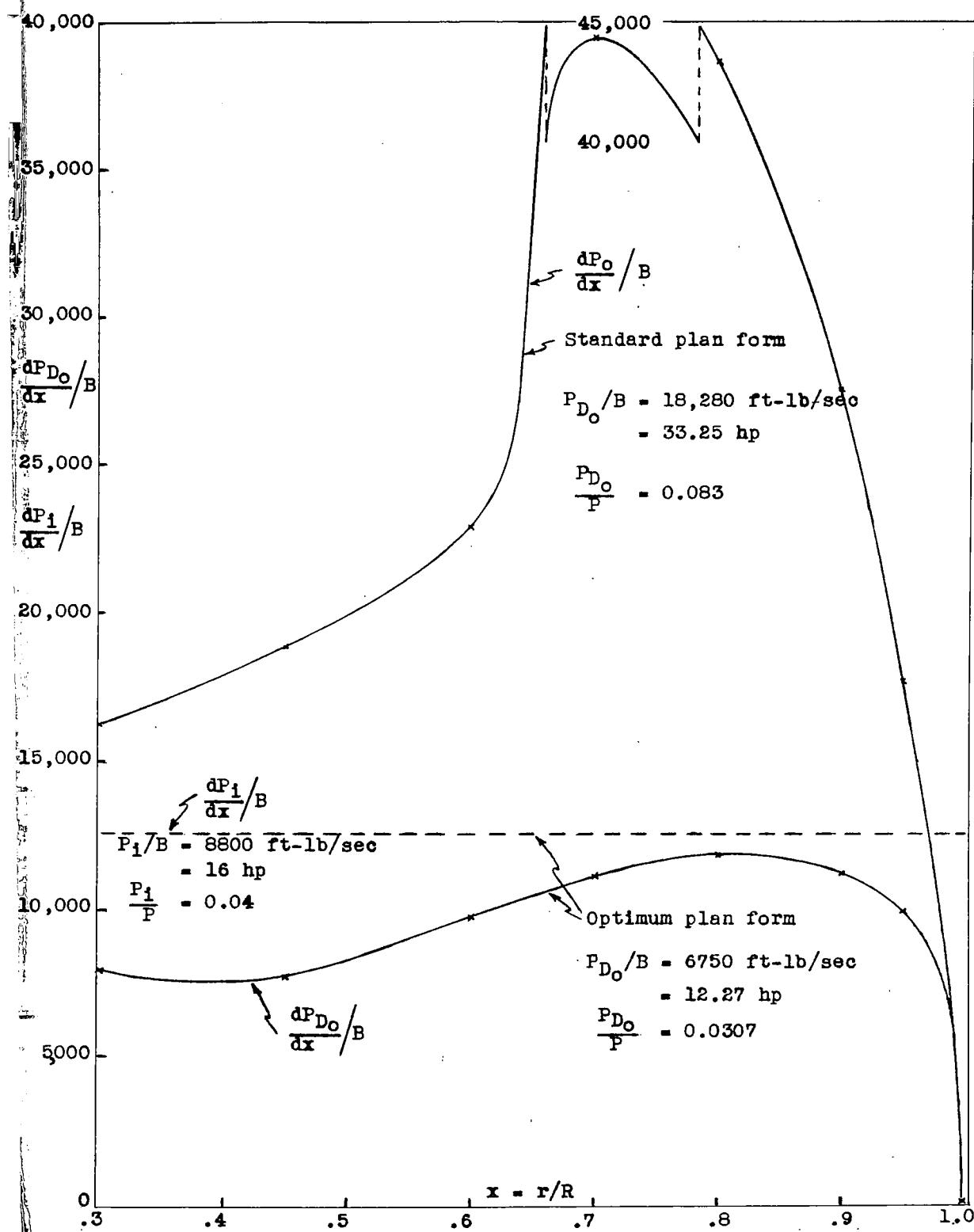
Figure 17.- Curves of power loss for two propellers.